Transcription Factors DksA and PsrA are synergistic contributors to *L. pneumophila* virulence in *Acathamoeba castellanii* protozoa

CHRISTOPHER I. GRAHAM, ANDREW J. GIERYS, TEASSA L. MACMARTIN, TIFFANY V. PENNER, JORDAN C. BECK, GERD PREHNA, TERESA R. DE KIEVIT and ANN KAREN C. BRASSINGA†

Department of Microbiology, Faculty of Science, University of Manitoba, Winnipeg, Manitoba, Canada R3T 2N2

Running Title: Regulatory synergy of DksA and PsrA in *L. pneumophila*

Keywords: *L. pneumophila*, stringent response, regulatory network, transcription factor, host-microbe interaction, biphasic lifestyle

†Corresponding author: Dr. Ann Karen C. Brassinga
Department of Microbiology (Fort Garry Campus)
Room 213, Buller Building
45 Chancellor's Circle
University of Manitoba
Winnipeg, MB, Canada
R3T 2N2
Phone: (204) 799-8457
E-mail: Ann.Brassinga@umanitoba.ca

Abstract

The environmental bacterium *Legionella pneumophila*, an intracellular parasite of free-living freshwater protozoa as well as an opportunistic human pathogen, has a biphasic lifestyle. The switch from the vegetative replicative form to the environmentally resilient transmissive phase form is governed by a complex stringent response-based regulatory network that includes RNA polymerase co-factor DksA. Here we report that, through a dysfunctional DksA mutation (DksA1), a synergistic interplay was discovered between DksA and transcription regulator PsrA. In *Acanthamoeba castellanii* protozoa, the presence of DksA1 ensured optimal intracellular growth, whereas PsrA could partially rescue the growth defect of the *dksA1* strain. Conversely, overproduction of DksA rescued the growth defect of a Δ*psrA* strain. Observed *in vitro*; either DksA or DksA1 were required for extended culturability of bacterial cells in depleted broth, but normal cell morphology and pigmentation required DksA only. Comparative structural modeling predicts that the DksA1 mutation affects coordination of Mg^{2+} into the active site of RNAP compromising transcription efficiency. Taken together, we propose that PsrA transcriptionally assists DksA. Additionally, *in vitro* evidence suggests that the long chain fatty chain metabolic response is mediated by PsrA together with DksA inferring a novel regulatory link to the stringent response pathway.

Introduction

Legionella pneumophila, a Gram-negative gammaproteobacterium, is commonly found in piped water distribution systems where it is found as an intracellular parasite of free-living bacterivorous protozoa (Rowbowtham, 1986; Steinert *et al.,* 2002; Newton *et al.,* 2010). These environments are not only amenable to bacterial colonization and proliferation, but can also aerosolize *Legionella*-laden water droplets that can be inhaled by susceptible individuals, thereby facilitating bacterial infection of alveolar macrophages resulting in the atypical pneumonia Legionnaires' disease (Newton *et al.,* 2010; Oliva *et al.,* 2018; Mondino *et al.,* 2020).

L. pneumophila is well adapted for its intracellular lifestyle in protozoa, and these adaptations also enable human infection due to highly conserved eukaryotic cellular biology (Newton *et al.,* 2010; Mondino *et al.,* 2020). A core driver of infection is the Dot/Icm Type IV secretion system (T4SS); an apparatus that enables secretion of a diverse repertoire of ≥ 330 effectors into the host cytoplasm that together act to modify host cellular physiology upon uptake of the bacteria (Finsel and Hilbi, 2015; Burstein *et al*., 2016; Gomez-Valero *et al.,* 2019). Such modifications include subversion of phagosome trafficking to prevent fusion of the bacteria-containing phagosome with lysosomes, and conversion of the phagosome into a replicative niche referred to as the *Legionella*-containing vacuole (LCV) (Tilney *et al.,* 2001; Kagan and Roy, 2002; Isberg *et al*., 2009). As infection progresses within a protozoan host cell, *L. pneumophila* exhibits a biphasic lifecycle, alternating between a vegetative replicative phase (RP) forms found primarily in the LCV, and transmissive phase (TP) forms that develop upon depletion of host-derived nutrients in anticipation of bacterial release to the environment. The physiology and ultrastructure of TP cells is optimized for environmental survival and resistance to stress, with expressed virulence factors enabling infection of a new host (Molofsky and Swanson, 2004;

Oliva *et al.*, 2018). In protozoa such as *Acanthamoeba castellanii*, TP cells were observed to be pleomorphic and eventually matured into highly infectious cyst-like forms with thickened cell walls, multiple membrane laminations and poly-β-hydroxybutyrate (PHB) granules (Faulkner *et al.*, 2002; Garduño *et al.*, 2002; Abdelhady and Garduño, 2013; Robertson *et al*., 2014). Development of cyst-like forms has not been observed in human macrophages, likely explaining the near-complete lack of human-to-human transmission (Abdelhady and Garduño, 2013).

The biphasic switch between RP and TP is controlled by a stringent response-based regulatory network activated by accumulation of alarmone guanosine tetraphosphate (ppGpp), which is synthesized by RelA and SpoT in response to nutritional deprivation. Synthase RelA senses low amino acid concentrations (Zusman *et al.*, 2002), whereas bifunctional synthase and hydrolase SpoT senses fatty acid flux via acyl carrier proteins (ACP) (Edwards *et al.*, 2009; Dalebroux *et al.*, 2010). Accumulated ppGpp is associated with activation of the LetA/LetS two component system (TCS), which in turn induces transcription of non-coding RNAs (ncRNAs) RsmY and RsmZ (Hammer *et al.*, 2002; Rasis and Segal, 2009; Sahr *et al.*, 2009; Nevo *et al.*, 2014). These ncRNAs target and sequester the RNA-binding protein CsrA, thus modulating CsrA-mediated post-transcriptional regulation of transcripts associated with the transition to TP. Such transcripts include those encoding Dot/Icm effectors and those linked to cellular metabolism (Häuslein *et al.*, 2017*;* Sahr *et al*., 2017). Other TCS also play a pivotal role in bacterial differentiation and are often required for virulence in host cells, such as CpxR/A (Feldheim *et al.*, 2016; Tanner *et al.*, 2016); PmrA/B (Zusman *et al.*, 2007; Al-Khodor *et al.*, 2009) and quorum sensing via LqsS/T/R (Tiaden *et al.*, 2007; Tiaden *et al.*, 2008; Schell *et al.*, 2014; Personnic *et al.*, 2018). In addition, a subset of transcriptional regulators plays an important role in TP induction. IHF assists LetA in the upregulation of RsmY and RsmZ, and is

required for full cyst-like form differentiation and virulence in *A. castellanii* (Morash *et al*., 2009; Pitre *et al*., 2013). OxyR regulates transcription of the operon encoding the CpxR/A TCS, linking it to virulence in *A. castellanii* (Tanner *et al.,* 2017). Recently, the autorepressor PsrA was found to be required for optimal intracellular growth and cyst-like form biogenesis in *A. castellanii* (Graham *et al*., 2021). While the genetic targets of PsrA have not yet been identified, a potential linkage between PsrA and the core stringent response network has been described with focus on fatty acid flux and an associated ACP (Graham *et al.,* 2021).

Accumulated ppGpp also directly affects transcriptomic changes associated with the transition from RP to TP. For example, expression of stationary phase sigma factor RpoS is increased (Dalebroux *et al*., 2010), which is required for the expression of TP traits and intracellular growth in protozoa such as *A. castellanii* (Hales and Shuman, 1999; Bachman and Swanson, 2001; Zusman *et al.,* 2002; Abu Zant *et al.,* 2006; Hovel-Miner *et al.,* 2009). While the precise mechanism has not yet been ascertained in *L. pneumophila*, ppGpp influences expression most likely by binding directly to RNA polymerase (RNAP), as has been described in *E. coli* where ppGpp binds with equal affinity either to a site encompassed by the ω and β' subunits, or at the interface between RNAP and secondary channel co-factor DksA. DksA features a pair of conserved aspartate residues to enable ppGpp binding (Perederina *et al.,* 2004; Ross *et al*., 2013; Ross *et al*., 2016; Myers *et al*., 2020). The latter event results in a conformational change in both ppGpp and DksA affecting the stability of the open complex generated by the RNAP holoenzyme thereby altering the efficiency of transcription initiation (Chatterji *et al*., 1998; Lemke *et al.,* 2011; Gummesson *et al.,* 2013; Ross *et al*., 2016; Molodtsov *et al.,* 2018; Travis and Schumacher, 2021). DksA can act independently of ppGpp, compensate for its absence if overexpressed, or even act antagonistically to ppGpp at different promoters (Magnussun *et al.,*

2007; Aberg *et al.*, 2008; Potrykus and Cashel, 2008; Aberg *et al*., 2009). DksA exists in a dynamic equilibrium with structural homologs GreA and GreB in *E. coli*, which compete with DksA for secondary channel binding; if either GreA or GreB binds then DksA-independent ppGpp binding to RNAP still occurs to influence expression (Vinella *et al.*, 2012).

L. pneumophila encodes both GreA and DksA orthologs, although *L. pneumophila* has not been targeted for study. Like its *E. coli* ortholog, DksA acts independently of, or in coordination with, ppGpp to regulate genes encoding TP traits (Dalebroux *et al.*, 2010). Previously, DksA was shown to be required in a ppGpp-dependent manner for TP morphogenesis including TP-specific flagellar biosynthesis. Likewise, DksA and ppGpp are both required for optimal intracellular growth in *A. castellanii*. Conversely, DksA, but not ppGpp, is dispensable for intracellular growth in murine macrophages, indicating that ppGpp may act independently of DksA in *L. pneumophila* (Dalebroux *et al.*, 2010). Thus, the contributions of ppGpp and DksA to the stringent response, are well characterized among the proteobacteria though the mechanisms and targets may vary between them (Gourse *et al*., 2018).

In this study, we describe a functional relationship between DksA and PsrA in regulation of virulence in protozoa, discovered fortuitously via a spontaneous secondary mutation within *dksA* in a Δ*psrA* strain background. The *dksA1* mutation was an in-frame deletion of a 24-base pair region that when expressed, produced a truncated but partially functional protein driving a unique phenotype. Through a combination of investigative approaches, we show that PsrA and DksA have distinct and overlapping biological roles in the regulation of TP. Incomplete suppression of phenotypes suggests that PsrA acts in a more targeted manner than DksA, and when interpreted alongside the unusual characteristics of the *dksA1* mutant, infers a high level of

regulatory complexity. Taken together, our findings illustrate a complex regulatory interaction between these two proteins, that together act to drive transmissive phase in *L. pneumophila.*

Results

Spontaneous *dksA1* mutation in Δ*psrA* strain In a previous study, we deleted *psrA* from the parental *L. pneumophila* Lp02 strain (Graham et al., 2021). Throughout this process, we noted a propensity for some of the isogenic Δ*psrA* strains to acquire secondary mutations in *letS* or *dksA* as discovered through routine whole genome sequencing. One particular Δ*psrA* strain was found to contain an in-frame 24 bp deletion located partway through the *dksA* coding sequence, that resulted in the loss of eight amino acid residues after the 57th residue in the DksA polypeptide. The 57th codon was additionally altered from encoding leucine to phenylalanine. This allele was denoted as the *dksA1* mutation that is characterized in this study (Figure S1A, B).

As the truncation appeared in the coiled-coil (CC) domain of DksA, we investigated how the truncation could affect the fold of DksA1 using AlphaFold2 (Jumper *et al*., 2021; Skolnick *et al*., 2021). Both DksA and DksA1 were submitted to the colabfold2 server (AlphaFold2) with default settings and were modelled with a moderate-to-high degree of confidence (Figure S1C, D). The CC domain of DksA was well built as was the majority of the globular-head (GH) domain. Conversely, the eight-amino acid truncation in DksA1 resulted in a partial disruption of the tip of the CC domain with AlphaFold predicting a ‘disordered’ loop with moderate confidence (Figure S1D). The extent of the potential structural changes in the mis-formed tip of the CC domain in DksA1 can be observed when overlayed with a previously solved structure of a DksA:RNAP complex from *E. coli* (PDB ID: 5VSW) (Molodtsov *et al*., 2018). As shown in Figure 1A, all DksA variants align well, except for the altered CC-loop regions near helix α3 and the C-terminal region helix α5 not present in the DksA *E. coli* crystal structure. Importantly, the truncation did not delete key function residues shown to be needed for interaction of DksA with the RNAP allosteric (K104, L101, K100, R97) or with the RNAP active site (D80, D77) (Parshin *et al*., 2015; Molodtsov *et al*., 2018) (Figure 1B). Furthermore, all DksA variant structures can be

modeled into RNAP (Figure S2) slotting into the allosteric site (Figure 1C) and RNAP active site (Figure 1D) without significant variation from the experimental DksA structure. However, while the AlphaFold predictions for Lp02 DksA and DksA1 had a properly modeled ppGpp binding site (Figure 1E), the twin-aspartate loop of the CC domain was significantly altered in DksA1 through the shift of D69 (D71 in DksA) by ~8.9Å (Figure 1F). These models therefore suggest that while the functional residues are conserved from the truncation, DksA1 should be incapable of coordinating the Mg^{2+} in the active site of RNAP. Conversely, the structural predictions show that DksA1 is likely still able to bind RNAP. Specifically, DksA1 is predicted to still contact the secondary binding site of ppGpp functionally as an allosteric inhibitor of RNAP through ppGpp mediated recruitment.

PsrA partially rescues the growth defect of the *dksA1*, but not Δ*dksA*, strain in *A. castellanii*

Given the previously described regulatory roles of DksA and PsrA (Dalebroux *et al.*, 2010; Graham *et al.*, 2021), the discovery of the Δ*psrA dksA1* mutant strain, and in turn the backtracked ancestral *dksA1* mutant strain, presented a fortuitous opportunity to investigate potential genetic links between the two regulatory factors in the established protozoan infection model *A. castellanii*. To test our hypothesis, we electroporated the *in trans psrA* expression vector (originally referred to as pComp in Graham *et al*., [2021] henceforth renamed to pComp-*psrA* in this study), or empty control vector pThy, into the mutant strains. Intracellular growth kinetics were conducted on *dksA1* pThy, Δ*psrA* pThy, *dksA1* Δ*psrA* pThy, and *dksA1* pComp-*psrA* strains, along with virulent Lp02 pThy and avirulent Δ*dotA* pThy strains as controls, at 25ºC over 168 h as previously described (Tanner *et al.*, 2016; Graham *et al*., 2021) (Figure 2A). The profiles of Lp02 pThy and Δ*dotA* pThy strains were as expected demonstrating ~ three-$\log_{10}$

increases in titre, and titres staying near initial inoculum density, respectively. The *dksA1* pThy and Δ*psrA dksA1* pThy strains showed no significant increase in titres indicating that the chromosomal single copy *dksA1* mutation was defective for virulence. Surprisingly, PsrA overexpression in the *dksA1* background resulted in a two-$\log_{10}$ recovery of growth ($p = 0.0006$) to a titre within one-$\log_{10}$ of the Lp02 pThy strain. This suggested that elevated levels of PsrA were able to partially, but not fully, rescue the avirulent phenotype demonstrated by the *dksA1* strain. While a genomic copy of *psrA* is present in the *dksA1* strain, it was shown previously that *in trans* overexpression of PsrA from pComp-*psrA* resulted in an elevated quantity of cellular protein that not only rescued the reduced growth phenotype associated with gene deletion of *psrA*, but also enhanced replicative growth of Lp02 in *A. castellanii* (Graham *et al.*, 2021). Nevertheless, the surprising ability of PsrA to partially complement the growth defect of *dksA1* led us to expand our investigations to define the relationship between the two regulatory factors.

A previous study elsewhere reported that an insertional *dksA* mutant showed a modest intracellular growth defect in *A. castellanii* at 37°C with slow growth initially, but eventually achieving similar titres to parental Lp02 by the end of the 96 h experiment (Dalebroux *et al,* 2010). This reported phenotype differs in comparison to the significantly reduced intracellular growth observed with the *dksA1* strain in this study. This difference supported our hypothesis that the truncated DksA1 protein bore altered function and distinct phenotype versus the null mutant. To further test this hypothesis, and to determine if the compensatory effect of *psrA* observed with the *dksA1* mutant strain extended to a null deletion mutant strain, we generated an unmarked, in-frame Δ*dksA* isogenic strain, as well as the double Δ*dksA* Δ*psrA* mutant strain. Complementation of DksA was achieved by cloning *dksA* and its native promoter into pJB908 creating pComp-*dksA* for electroporation into the Δ*dksA* strain. Plasmid pComp-*psrA* was also

electroporated into the Δ*dksA* strain to test if the rescue of the growth defect in *dksA1* by PsrA overexpression was reproducible. Empty control vector pThy were electroporated into both Δ*dksA* and Δ*dksA* Δ*psrA* strains. The intracellular growth kinetics of the generated strains were assessed in *A. castellanii* under the same conditions as before along with Lp02 pThyA and Δ*dotA* pThyA as control strains (Figure 2B). Interestingly, the single Δ*dksA* pThy and double Δ*dksA* Δ*psrA* pThy mutant strains were both fully avirulent, starting at a slightly lower titre than the Δ*dotA* pThy strain, then declining to, or below, the detection limit of the assay (~10 CFU/mL). The severe growth defect of the Δ*dksA* pThy strain was fully rescued by *in trans* expression of *dksA*, but not *psrA*; a notable divergence from the rescued phenotype demonstrated by the *dksA1* pComp-*psrA* strain. Taken together, the lack of DksA results in a complete avirulent phenotype in these conditions which cannot be rescued by PsrA, whereas the partially functional DskA1 has a less severe impact on intracellular growth that can be partially rescued by PsrA.

DksA1 rescues the growth defect of the Δ*dksA* strain, and vice versa, in *A. castellanii* Given that DksA can rescue the severe growth defect of the Δ*dksA* strain in *A. castellanii* (Figure. 2B), we next asked if the partially functional DksA1 could likewise do so despite the truncation in the coiled-coil structure (Figure 1). To this end, the *dksA1* gene and its native promoter was cloned from the *dksA1* genome into pJB908, creating pComp-*dksA1*, which was electroporated into Δ*dksA* to generate the Δ*dksA* pComp-*dksA1* strain for assessment in *A. castellanii*, along with Δ*dksA* pThy, and Lp02 pThy and Δ*dotA* pThy as control strains (Figure 2C). The severely reduced growth phenotype of the Δ*dksA* pThy strain was robustly rescued as by *in trans* complementation with DksA1 as shown by the growth profile of the Δ*dksA* pComp-*dksA1* strain (p = 0.0002) matching that of the Lp02 pThy strain. It should be noted that this growth

phenotype contrasted with the minimal growth profile of the Δ*dksA1* pThy strain (Figure 2A), suggesting that restoration of the virulent phenotype of the Δ*dksA* strain was due to plasmid-copy number driven overproduction of DksA1 protein (pComp-*dksA1*), sufficient to offset the structural and functional inefficiency caused by the intragenic 24 bp deletion. Not unexpectantly, *in trans* complementation of DksA successfully rescued the avirulent phenotype of the *dksA1* pThy strain to match the growth profile of Lp02 pThy as the plasmid-copy number driven production of DksA outnumbered that of DksA1 (Figure 2D). In the reverse scenario, the growth profile of Lp02 pComp-*dksA1* still matched that of Lp02 pThy suggesting that despite the plasmid-copy number driven production of DksA1, the chromosomal-copy production levels of DksA and PsrA in parallel were each sufficient to disguise any effects caused by the dysfunctional DksA1 (Figure 2A, Figure 2D).

DksA restores the growth defect of the Δ*psrA* strain in *A. castellanii* To further define the relationship between DksA and PsrA, we next asked if DksA could reciprocally compensate for lack of PsrA or generally, affect intracellular growth in the presence of PsrA. To this end, pComp-*dksA* was electroporated into parental Lp02 and Δ*psrA* strains and then assessed for growth in *A. castellanii* along with the Lp02 pThy and Δ*dotA* pThy strains as controls, and the Δ*psrA* pThy strain for comparative purposes (Figure 2E). As previously reported, the Δ*psrA* pThy strain consistently maintained 1 $\log_{10}$ lower than that of Lp02 pThy (p = 0.029) (Graham *et al*., 2021). The mean growth profile of the overexpression Lp02 pComp-*dksA* strain showed a subtle increase of ~½ $\log_{10}$ over that of Lp02 pThy (p = 0.007); this enhancement could also be seen in the Δ*dksA* pComp-*dksA* complemented strain (Figure 2D; p = 0.0247). Likewise, we found that *in trans* expression of DksA in the Δ*psrA* pComp-*dksA* strain rescued the growth

defect of Δ*psrA* strain, increasing growth by ~1 $\log_{10}$ to match that of Lp02 pThy strain ($p < 0.001$ versus Δ*psrA* pThy, not significant versus Lp02 pThy). Although this experiment did not generate large phenotypic differences, we found the tendency towards subtle phenotypes upon *in trans* expression of DksA to be noteworthy relative to the very strong phenotypes noted in the *dksA* mutant strains.

DksA is not required for intracellular growth in human U937-derived macrophages

Some *L. pneumophila* genes exhibit host specific requirements; being required only for growth in one host type, but not in another. Previous work with *L. pneumophila* showed that the human U937-derived macrophage host model is more permissive to regulatory mutants than *A. castellanii*, as exemplified by transcriptional regulator Δ*psrA* or Δ*cpxRA* TCS mutants (Tanner *et al.*, 2016; Graham *et al.*, 2021). DksA was previously shown to be dispensable for growth in primary murine bone marrow macrophages (Dalebroux *et al.*, 2010); however, since the phenotype we observed for a Δ*dksA* strain in *A. castellanii* was different from that reported by Dalebroux *et al*. (2010), we decided to verify the phenotype in mammalian macrophages. Intracellular growth kinetics were assessed for the same set of strains used in the *A. castellanii* infection assays (Figure 2) in the human U937-derived macrophage infection model. As expected, positive control Lp02 pThy grew well, increasing approximately 100-fold by the 72 h timepoint (Figure 3A), and negative control Δ*dotA* pThy maintained a steady titre with no growth. In comparison to that of Lp02 pThy, Δ*dksA* pThy and *ΔdksA ΔpsrA* pThy strains showed similarly robust, but offset (delayed) growth profiles. Additionally, despite normalization of the inoculum by OD_{600}, these two strains showed initial measured titres lower than that of Lp02 pThy (Figure 3A). Only *ΔdksA ΔpsrA* pThy showed a significant deviation from the parental

strain ($p = 0.049$). The Δ*dksA* pComp-*psrA* showed a similar profile to the parental strain (Figure 3A), and did not show the reduced starting titre, but the difference to Δ*dksA* pThy was not significant. No significant change in phenotype was observed with the remaining set of strains featuring *in trans* DksA expression, either by complementation (Δ*dksA* pComp-*dksA*), overexpression, (Lp02 pComp-*dksA*) or in Δ*psrA* pComp-*dksA* (Figure 3B). The growth profiles of the *dksA1* pThy, *dks1* Δ*psrA* pThy, or *dksA1* pComp-*psrA* were indistinguishable from Lp02 pThy (Figure 3C) and lacked even variability in the initial uptake. Thus, these results verify that DksA is not required for, nor does it enhance, intracellular growth in mammalian macrophages.

***In vitro* growth is impacted by DksA, PsrA and DksA1** The differences observed with the intracellular growth kinetics of isogenic mutant and complemented strains in *A. castellanii* may be in part due to defects in the growth rates of the cells, rather than solely virulence defects *in vivo*. To distinguish this possibility and more generally characterize the *in vitro* growth characteristics of the strains, we tested the *in vitro* growth rates of the strains in BYE broth at 37ºC over a 24-hour time period (Figure 4). The growth profiles of the first set of strains (*dksA1* pThy, *dksA1* Δ*psrA* pThy, *dksA1* pComp-*psrA*, *dksA1* pComp-*dksA*) (Figure 4A) were similar to each other, and to that of Lp02 pThy. The growth profiles of the second set of strains (Δ*psrA* pThy, *psrA* pComp-*dksA*, Lp02 pComp-*dksA*, Lp02 pComp-*dksA1*) were slightly varied. Consistent with our previous study, the growth profile of Δ*psrA* pThy was significantly reduced in comparison to that of Lp02 pThy ($p = 0.036$; Figure 3B) (Graham *et al*., 2021). For the DksA overexpression Lp02 pComp-*dksA* and DksA-complemented Δ*psrA* pComp-*dksA* strains, plasmid-driven overproduction of DksA seemed to slightly reduce the growth profiles in comparison to the growth profiles of Lp02 pThy and Δ*psrA* pThy, respectively (both $p < 0.001$;

Figure 4B). Conversely, overexpression of DksA1 had no effect as the growth profiles of Lp02 pComp-*dksA1* and Lp02 pThy were similar.

Interestingly, the *in vitro* growth kinetics of Δ*dksA*-based strains featured a phenotype of growth variability across replicates as manifested by the large error bars for hourly data points (Figures 4C, 4D). This growth variability made the determination of statistical significance difficult when comparing growth profiles of mutant and/or complemented strains to that of Lp02 pThy. This is exemplified by the growth profiles of Δ*dksA* pThy and Δ*dksA* Δ*psrA* pThy strains of which both appeared to be elevated in comparison to that of Lp02 pThy (Figure 4C), but the difference was not statistically significant. This variability is also seen with the Δ*dksA* pComp-*psrA* and Δ*dksA* pComp-*dksA1* growth profiles, with the former not rescued and the latter generating a growth profile significantly reduced in comparison to that of Lp02 pThy ($p < 0.0001$; Figure 4C). Notably, the growth variability disappeared from the Δ*dksA* pComp-*dksA* growth profile suggesting this was a complementable phenomenon. The growth additionally was slightly reduced in comparison to that of Lp02 pThy ($p=0.017$), likely due to plasmid-copy number driven overproduction of DksA. Conversely, the DksA1 overexpression Lp02 pComp-*dksA1* strain produced a growth profile matching that of the parental Lp02 pThy strain (Figure 4B) with minimal growth variability across replicates. This suggests that elevated levels of DksA1 imparts a negative effect on replicative growth in absence of the parental *dksA* allele.

The *in vitro* growth profile assays were repeated at 25°C, albeit over a 48-hour time period to account for the slower growth rate, to mimic the incubation temperature of the *A. castellanii* assays. The resultant growth profiles were mostly similar to those attained at 37°C, with growth variability of strains lacking *dksA* exacerbated at 25°C as indicated by data points with widened error bars (Figure 5). One notable difference was that the growth profile of Δ*dksA*

pComp-*dksA1* strain matched that of Lp02 pThy at 25°C (Figure 5C), versus the reduction at 37°C (Figure 4C), suggesting that the slower growth rate and/or lower temperature accommodated the dysfunctional nature of DskA1.

These findings together suggest that while strains lacking *dksA* featured more variability in growth profiles, more so at 25°C then at 37°C, the *in vitro* growth assays (Figures 4 and 5) illustrates that the observed *in vivo* growth defects are specific to *A. castellanii* (Figure 2), and not due to poor growth of the bacterial cells themselves.

DksA, and possibly PsrA, mediates cell morphology Throughout this study, it was noted that the colony morphologies of Δ*dksA* and *dksA1* strains grown on BCYE agar plates differed significantly from that of parental Lp02. In comparison to the opaque beige-white glossy colonies with varied margins featured by Lp02, Δ*dksA* colonies were textured glossy white with defined margins, and *dksA1* colonies were smooth glossy white with defined margins. The phenotypes were particularly evident when 10 µL of OD_{600} = 0.15 bacterial suspensions in broth were spotted onto BCYE plates as were done in serial dilution assays in this study (Figure 6). For both Δ*dksA* and *dksA1* strains, the phenotype was fully rescued by *in trans* complementation of DksA whereas *in trans* DksA1 complementation partially rescued Δ*dksA*. The colony morphology of the Δ*dksA* Δ*psrA* was similar to that of the Δ*dksA* strain, but not to the Δ*psrA* strain which was similar to that of the parental strain indicating the sole influence of DksA. Finally, *in trans* PsrA complementation did not appear to alter colony morphology in all strain backgrounds assessed (Lp02, Δ*dksA*, *dksA1*, Δ*psrA*), confirming that PsrA does not influence this phenotype.

We previously reported that PsrA promoted cell elongation when overexpressed *in trans* (Graham *et al.*, 2021). Conversely, it was reported elsewhere that lack of DksA influenced cell elongation (Dalebroux *et al*., 2010). To assess whether a genetic relationship between PsrA and DksA was evident in cell structure morphology, and to further explore whether *dksA1* generated a phenotype distinct from Δ*dksA*, bacteria were inoculated into BYE broth from OD_{600} = 0.02 and grown overnight to OD_{600} = ~0.5, (exponential growth phase; EP), or another 24 h beyond (stationary phase; SP) respectively, for microscopic analyses (Figure 7). Cell lengths were quantified by measuring cells with the length tool in ImageJ and plotted separately for analysis (Figures 8A and 8B). As a control, Lp02 pThy bacteria formed typical rods (mean length 3.6 µm) in EP, that elongated into SP (mean length 5.8 µm). The Δ*dksA* pThy bacteria were notably elongated in EP (mean length 6.2 µm) and, in SP, became extremely elongated into filamentous forms often of sufficient length to often exceed the field of view, averaging 13.2 µm among measurable cells (with the entire cell visible in one field of view). Likewise, the Δ*dksA* Δ*psrA* pThy bacteria were also elongated in EP, and strongly filamentous in SP (mean lengths 5.4 µm and 17.1 µm, respectively). Conversely, Δ*psrA* pThy bacteria were morphologically indistinguishable to Lp02 pThy, as previously observed (Graham *et al*, 2021). The Δ*dksA* pComp-*dksA* bacterial forms resembled those of Lp02 pThy indicating that filamentation was rescued by DksA complementation: they were slightly but significantly shortened relative to Lp02 (2.9 µm and 4.7 µm in EP and SP phases, respectively). Expression of DksA *in trans* in Δ*psrA* pComp-*dksA* and Lp02 pComp-*dksA* strains also resulted in slightly, but significantly shorter cell lengths in comparison to those of Lp02 pThy and comparable to Δ*dksA* pComp-*dksA* in both growth phases, suggesting the shortening mediated by DksA is independent of PsrA.

PsrA complementation in Δ*dksA* pComp-*psrA* did not strongly affect the bacterial cell lengths and elongation was still present (7.5 µm and 14.2 µm in EP and SP, respectively).

Conversely, the *dksA1* pThy, *dksA1 ΔpsrA* pThy, and *dksA1* pComp-*psrA* were slightly elongated relatively to parental Lp02 pThy in both EP (5.0 µm, 5.1 µm and 4.3 µm, respectively) and SP (7.5 µm, 7.7 µm, and 7.8 µm, respectively) but were not filamentous, and did not vary significantly from each other again supporting the hypothesis that the *dksA1* allele maintained partial function. Interestingly, the Δ*dksA* pComp-*dksA1* strain did not show complementation of the elongation to resemble *dksA1* levels as might be expected (5.6 µm in EP, 12.3 µm in SP). To rule out the simple possibility of the two gene products conflicting in some way, we tested *dksA1* pComp-*dksA*, that reversed the alleles expressed on plasmid and the chromosome, and this strain appeared somewhat shortened relative to parental Lp02 pThy in SP only (4.2 µm) resembling the other *in trans dksA* overexpression strains, suggesting that relative protein concentrations may drive the phenotype. Together, this indicates that the previously reported role of *psrA* is overshadowed by the more potent role of DksA, and that the DksA1 protein shows an intermediate phenotype illustrating that DksA1 is a partially functional protein in these strains.

DksA or DksA1 are necessary for extended culturability in depleted media Previously, the insertional Δ*dksA* strain was also noted to feature reduced recovery of culturable bacteria after extended incubation in depleted media, which the authors referred to as “survival” (Dalebroux *et al.*, 2010), although the assay attempted to recover culturable rather than viable bacteria. Over the course of this study, we noticed that the Δ*dksA* mutants could not be consistently sub-cultured (likely contributing to the variability of these strains seen in Figure 3), or often failed to grow entirely if taken from plates grown more than three days, ordinarily easily possible with

parental strains. In view of this, we asked if this was a consequence of previously observed culturability phenotype occurring in the unmarked Δ*dksA* mutant, and potentially the *dksA1* strains, and whether PsrA may also contribute. As this phenotype had not been assessed in the prior PsrA study (Graham *et al.*, 2021), we decided to include Δ*psrA* pThy, Δ*psrA* pComp-*psrA* and Lp02 pComp-*psrA* (*psrA* overexpression) strains from Graham *et al.* (2021). The bacteria from each strain were suspended in BYE at OD_{600} = 0.15, and grown at 37°C for 96 hours with shaking, with samples taken for optical density values and CFU/mL titres at 24 h intervals.

Over the time course, optical density values peaked comparably for all strains at 24 h, and held steadily to the 96 h timepoint (Figure 9). Enumeration of titres for Lp02 pThy and Δ*psrA* pThy were comparable to one another, but the titres for Δ*dksA* pThy and Δ*psrA* Δ*dksA* pThy were significantly reduced by 72 h, and more so by the 96 h for Δ*dksA* pThy, noting that titre enumeration was not possible for Δ*psrA* Δ*dksA* pThy at 96 h as no colonies were recovered in any replicate for this strain at that timepoint (detection limit ~10^2 CFU/mL; Figure 9A). The reduced culturability phenotype was rescued by *in trans* complementation of DksA or DksA1, but not PsrA (Figures 9B, 9C). The extended culturability of *dksA1* pThy strain was unaffected in comparison to parental Lp02 pThy, thereby not requiring nor significantly benefiting from plasmid-borne *in trans* complementation of DksA (Figure 9D). The unaltered phenotype of *dskA1* Δ*psrA* pThy and Δ*psrA* pComp-*dksA* strains further supports the observation that PsrA does not contribute to, nor does overexpression of DksA (i.e. Lp02 *pComp-dksA*) significantly improve, extended culturability (Figures 9E, 9F). Thus, in summary, PsrA plays no role in extended culturability, while DksA is essential for the culturability of Lp02 in depleted media as reported elsewhere previously (Dalebroux *et al.*, 2010). Notably, the hypomorph *dskA1* allele has retained this essential function of promoting extended culturability.

Pigmentation requires fully functional DksA, but not PsrA *L. pneumophila* pigment is a brown, melanin-like secreted protein that is released into the supernatant during the transition to stationary phase under the control of the stringent response through RelA (Zusman *et al*., 2002; Dalebroux *et al.*, 2010). Further, we observed hyperpigmentation of a subset of parental, isogenic (Δ*psrA*, Δ*dksA*) and *dksA1* strains overproducing *dksA in trans* (Figure 10A). To ascertain whether DksA1 and/or PsrA could contribute to this hyperpigmentation, we quantified the pigmentation for each strain by measuring absorbance of the bacterial culture supernatant at 550 nm as done elsewhere (Wiater *et al.*, 1994; Dalebroux *et al.*, 2010) (Figure 10B).

The parental Lp02 pThy strain developed moderate pigmentation (Abs_{550}/OD_{600} = ~0.20) that was similarly achieved by Δ*psrA* pThy, Δ*psrA* pComp-*psrA*, and Lp02 pComp-*psrA* strains suggesting that PsrA does not influence pigmentation (Figure 10B). This supposition is further borne out by the significantly reduced pigmentation (Abs_{550}/OD_{600} = 0.10 - 0.12) featured by both of the Δ*dksA* Δ*psrA* pThy and Δ*dksA* pThy strains, which the latter is rescued to significantly increased levels (i.e. hyperpigmentation) (Abs_{550}/OD_{600} = 0.36 - 0.38) over that of Lp02 pThy likely due to plasmid-copy number driven overproduction of DksA (Figure 10B). Indeed, the pigmentation phenotype was rescued by *in trans* DksA complementation in the Δ*psrA* strain background, but not by *in trans* PsrA complementation in the Δ*dksA* strain background, clearly indicating that only DksA positively influences pigmentation (Figure 10B). Pigmentation was also significantly reduced (Abs_{550}/OD_{600} = 0.05 - 0.09) in the *dksA1* pThy and *dksA1* Δ*psrA* strain backgrounds, and the phenotype is not rescued by *in trans* PsrA complementation verifying the lack of involvement in pigmentation by PsrA (Figure 10B). Surprisingly, the hypomorph DksA1 could not rescue pigmentation in the Δ*dksA* strain, but pigmentation of *dksA1* strain could be induced by *in trans* DksA complementation. The *dksA1*

pComp-*dksA* strain showed delayed onset of hyperpigmentation such that only one of three replicates had fully pigmented by 30 h; all replicates of this strain pigmented by 48 h (Figure 10A), but at 30 h the difference was not statistically significant. These findings indicate that the ability of DksA1 to interact with RNAP is impaired as suggested by structural modelling (Figures 1, 10B). Taken together, these findings indicate that DksA is sufficient to drive pigmentation independent of PsrA, although, curiously the *dksA1* strain was unpigmented like the Δ*dksA* strain, which can be interpreted as the truncated region impacting this phenotype for more than, for example, extended culturability where no significant impact was observed.

Growth in long chain fatty acids is mediated by PsrA and DksA The activation of the biphasic switch is mediated in part by the response to fatty acid flux (Edwards *et al.*, 2009; Dalebroux *et al.*, 2010). It was shown elsewhere that *in vitro* supplementation of short chain fatty acids (SCFAs), such as propionic acid, will trigger the expression of transmissive phase traits (Edwards *et al.*, 2009). Further, the process of differentiation in response to excess SCFAs is mediated by DksA (Dalebroux *et al.*, 2010). Likewise, PsrA is associated with differentiation and although the precise role remains to be elucidated, the *Pseudomonas* PsrA ortholog is a sensor of long chain fatty acids (LCFAs), presence of which alleviates PsrA-mediated repression of the *fadBA5* β-oxidation operon (Kang *et al*., 2008). In this view, Δ*psrA* and complemented strains were grown in BYE broth supplemented with the LCFA, palmitic acid, to determine if bacterial growth was impacted by lack of PsrA. In comparison to normalized Lp02, 2-fold inhibition of growth of the Δ*psrA* pThy strain was observed which was rescued by *in trans* PsrA expression strongly suggesting the involvement of PsrA in responding to LCFAs (Figure 11A). Because chromosomal DksA expression is present in the Δ*psrA* pThy strain, we next asked if

DksA had a contributing factor in responding to palmitic acid which could be amplified through *in trans* DksA expression in the Δ*psrA* strain background. While it appears that growth of the Δ*psrA* pComp-*dksA* strain improved, it was not statistically significant (Figure 11A). Likewise, *in trans* DksA expression in the parental strain background did not significantly improve bacterial growth over that of the parental strain alone (Figure 11A). To further investigate the role of DksA, Δ*dksA*-based strains were assessed in palmitic acid-supplemented BYE media. As expected, the double Δ*dksA* Δ*psrA* pThy strain had 2-fold growth inhibition with less variability amongst the data points than in comparison to the Δ*psrA* pThy strain by itself (Figure 11A, 11B). Growth inhibition of the Δ*dksA* pThy strains was not considered statistically different from the normalized growth of Lp02 (Figure 11B). Conversely, *in trans* DksA expression significantly improved bacterial growth over that of normalized Lp02 (Figure 11B). Surprisingly, *in trans* PsrA expression in the Δ*dksA* strain background could not fully rescue the growth inhibition phenotype. Taken together, these results suggest that while PsrA is largely responsible for the response to LCFAs, DksA also contributes additively to this response lending support to the overlapping roles observed for the two regulatory factors for some of the traits in this study.

Discussion

The biphasic lifecycle of *L. pneumophila* is controlled by the convergence of multiple signals into a sophisticated regulatory network that ultimately acts to induce TP differentiation. The primary signals driving differentiation link to the nutritional status of the environment, mediated largely by induction of the stringent-response and the associated downstream regulatory network in association with RNAP-binding cofactor DksA, alternative sigma factor RpoS, two-component systems and a subset of transcriptional regulators including PsrA (Fonseca and Swanson, 2014; Oliva *et al*., 2018; Graham *et al*., 2024).

This study investigated a spontaneous *dksA* mutation, termed *dksA1*, resulting in a truncated DksA1 protein featuring a deletion within its CC domain (Figure 1) (Perederina *et al,* 2004; Dalebroux *et al.,* 2010). The Δ*dksA1* strain showed reduced intracellular growth in *A. castellanii* protozoa that was partially, but not fully, rescued by *in trans* expression of *psrA* allowing us to propose *dksA1* and encoded protein product as representing a partially functional allele whose phenotypes allowed us to explore overlapping cellular functions of both regulators, inferring an overlap of gene targets regulated by DksA and PsrA (Figure 2A).

The intermediate phenotype observed in bacteria expressing DksA1 relative to DksA can be explained by comparing their AlphaFold2 models to that of *E. coli* DksA bound to RNAP (Figure 1) (Molodtsov *et al*., 2018). These models predict DksA1 to be physically incapable of coordinating magnesium in the active site of RNAP due to the truncated loop in the CC domain (Figure 1D, F). However, DksA1 is still predicted to overall form the core CC and GH domains (Parshin *et al*., 2015; Molodtsov *et al*., 2018). This would hypothetically still allow DksA1 to bind into the allosteric binding pocket of RNAP (Figure 1C, S2) thereby recruiting a secondary ppGpp to RNAP. This would partially explain the variance in phenotype of *dksA1* as an intermediary between the WT and knockout strain. Likewise, these structural predictions also fit

into the model of the interplay between GreA and DksA as allosteric inhibitors/activators of RNAP competing for the same allosteric site (Parshin *et al*., 2015; Molodtsov *et al*., 2018).

To explore the possibilities that either DksA and PsrA genetically interact with each other, or act in parallel, Δ*dksA* and Δ*dksA* Δ*psrA* strains were subsequently assessed for growth kinetics in *A. castellanii* protozoa (Figure 2). The Δ*dksA* strain developed a more severely avirulent phenotype than the *dksA1* strain, and was rescued by *in trans* complementation of *dksA* and by *dksA1*, but not by *psrA*. Notably, the avirulent phenotype of the Δ*dksA* pThy strain contrasts to previous experiments showing that a Δ*dksA* insertional mutant strain exhibited reduced intracellular growth, but was not avirulent in *A. castellanii* (Dalebroux *et al.,* 2010). This discrepancy in findings could be due to differing experimental conditions as Dalebroux *et al.* (2010) conducted *A. castellanii* infections at 37°C. Temperature-dependent phenotypes have been seen previously, for example, with Δ*hfq* mutant strains, which only showed an intracellular kinetic defect in *A. castellanii* at 30°C, but not at 37°C (McNealy *et al.,* 2005). We undertook the *A. castellanii* infections at 25°C and showed that the avirulent phenotype of Δ*dksA* was fully complemented by *in trans* DksA expression (Δ*dksA* pComp-*dksA*) indicating that the phenotype was solely due to the genetic deletion of *dksA*. Another possibility for the discrepancy is the possibility of different deletion strategies causing polar effects; Sahr *et al* (2012) annotated *L. pneumophila* Paris strain *dksA* in an operon with an uncharacterized alpha/beta hydrolase *lpp2286* encoded downstream and Lp02-derivative strains are likely similar. However, both our study and the previous work by Dalebroux *et al* (2010) showed the respective mutants were complementable and thus, the discrepancy is unlikely a polar effect, although the previous work did not test this in their intracellular kinetics assay. Additionally, *in trans* expression of DksA1 was sufficient to compensate for lack of DksA indicating that the mutant truncation did not

impact essential function of DksA. Lastly, expression of DksA enhanced and rescued intracellular growth in Lp02 and Δ*psrA* strains, respectively. Thus, DksA can compensate for lack of PsrA, and PsrA can partially compensate for the reduced activity of DksA1, but cannot compensate for the absence of DksA intracellularly in *A. castellanii*. Taken together, the interplay of DksA and PsrA in regulating their gene targets is not fully reciprocal, indicating that successful intracellular growth in *A. castellanii* is largely driven by DksA with assistance from PsrA.

The requirement of DksA for intracellular growth is host specific. DksA was shown elsewhere to be dispensable for growth in primary murine macrophages (Dalebroux *et al*., 2010) and for human U937-derived human macrophages as shown in this study (Figure 3). Likewise, the Δ*dksA* Δ*psrA* strain was not impeded for intracellular growth in U937-derived macrophages; a finding similar to that previously found with the Δ*psrA* strain (Graham *et al*., 2021). Overexpression of DksA in the Lp02 strain background enhanced intracellular growth in protozoa, but with little overall impact in U937-derived macrophages, a trend also seen with overexpression of PsrA (Graham *et al*., 2021), indicating that elevated levels of either regulatory factor on an individual basis imbued a positive effect on replication in *A. castellanii* that did not equate to a substantial phenotype in U937-derived macrophages.

The induction of regulatory mechanisms controlling the transition switch from RP to TP are generally comparably induced *in vivo* (e.g. in protozoa) and *in vitro* (Byrne and Swanson, 1998), thus enabling *in vitro* approaches to examine growth kinetics and phenotypes characteristic of TP-associated traits of *L. pneumophila*. To this end, *in vitro* kinetic assays were undertaken to show the interplay between DksA and PsrA were largely growth temperature-independent (Figures 4 and 5). While the Δ*dksA* mutant strain featured erratic but generally

enhanced growth, incrementally increased *in trans* expression of DksA in Δ*dksA* and parental strains, respectively, inhibited growth in broth. This phenotype was inverse to that seen of the Δ*dksA* strain harboring chromosomal and *in trans* expression of PsrA which positively impacted growth within protozoa (Figure 2B). Moreover, the Δ*psrA* pComp-*dksA* strain grew slower than either Δ*psrA* or Lp02 pComp-*dksA* strains individually in broth, suggesting the presence of an additive effect (Figures 4D). The slowest growing strain in broth was Δ*dksA* pComp-*dksA1*, indicating that the mutant truncation bore functional consequence towards growth rates, a curious discrepancy when compared with the growth rate of this strain in protozoa, which resembled the parental Lp02 (Figures 2C, 4C). The slow *in vitro* growth phenotype did not apply to the *in vivo* grown Lp02 pComp-*dksA1* strain bearing chromosomally expressed DksA, inferring that DksA1 is not a dominant-negative allele (Figure 2D) and suggesting an underlying complexity to the altered function of the mutant protein. Taken together, the *in vitro* growth kinetic profiles were consistent with the current model of DksA promoting TP-associated traits (Dalebroux *et al.*, 2010).

Other phenotypes such as cellular filamentation, pigmentation, and recovery of culturable bacteria from depleted media, were consistent with previously reported findings (Dalebroux *et al.*, 2010). Lack of DksA resulted in unusual colony morphology (Figure 6) and elongated cell morphology (i.e., filamentation), particularly in stationary phase (Figures 7-8). Lack of DksA also dramatically reduced bacterial culturability upon extended incubation in depleted broth (Figure 9). Given the link to the stringent response, the Δ*dksA* strain may be physiologically poorly equipped to handle nutrient deprivation or other stressors found in depleted broth. Biologically, PsrA does not contribute to this phenotype. RNA-Seq analyses of Δ*psrA* or *in trans psrA* expression strains showed few stress-related genes under PsrA regulation (Graham *et al.*,

2021), so PsrA may be dispensable in these conditions. Further to this, filamentation and culturability likely influence DksA-dependent variability in optical density to titre ratios of stationary phase bacteria recovered from three-day old BCYE plates, and thus explain the variability in the *in vitro* growth curves, and potentially, the low inoculum titre in the *in vivo* kinetics. Indeed, DksA was recently ascertained to have a pivotal role in cell division in *E. coli*; binding of ppGpp to DksA/RNAP indirectly activates the divisome complex component FtsZ to modulate cell length and division (Anderson *et al*., 2023). The absence of either DksA or ppGpp promotes cell filamentation for different reasons; lack of DksA prevents activation of cell division by ppGpp resulting whereas lack of ppGpp causes DksA to switch from an activator to an inhibitor of FtsZ. Thus, by orthologous function, it is likely that DksA behaves in the same manner in *L. pneumophila* as Δ*dksA* cells are filamentous (Figures 7 and 8) (Dalebroux *et al.*, 2010). Lastly, pigmentation comprises a brown tyrosine-based metabolite produced post-exponentially by *L. pneumophila* as an adaptation to environmental stress, potentially serving for photoprotection, iron acquisition, or as a biocide to enhance *L. pneumophila* competitiveness in biofilms (Steinert *et al.*, 1995; Chatfield and Cianciotto, 2017; Levin *et al.*, 2019). As reported elsewhere, DksA is a major driver of pigment production (Figure 10) (Dalebroux *et al.*, 2010). Conversely, these traits, other than cell length, do not seem measurably impacted by the cellular levels of PsrA, indicating that PsrA may impact virulence specific pathways rather than cellular physiology.

Fatty acid flux is linked to *L. pneumophila* TP differentiation through SpoT-mediated stringent induction, with either DksA or ppGpp, sufficient to arrest growth upon supplementation with SCFA (Edwards *et al.*, 2009; Dalebroux *et al.*, 2010). Here, we show that like its ortholog in *Pseudomonas* spp., PsrA is responsive to fatty acids suggesting a conserved functional role in

sensing LCFA in the environment alongside SpoT, and further, both DksA and PsrA must be present to ensure a proper LCFA response (Figure 11) (Kang *et al.*, 2008), although the mechanistic details of the PsrA-mediated response remain undefined until further study can be undertaken.

Together, our findings show that the truncation in DksA1 affects different biological processes in different ways, with phenotypes of *dksA1* strains ranging from identical to the parental strain, to identical to that of the full Δ*dksA* mutant, or intermediate to either, illustrating that the dysfunctional DksA1 may impact different cellular processes in different ways given the wide disparities in phenotypes attributed to this allele. As the functional basis of the *dksA1* phenotype has not been elucidated, these results cannot distinguish the distinct effects of ppGpp recruitment and competitive sequestration of RNAP from GreA; the presence of multiple DksA-mediated regulatory mechanisms could contribute to the variability of phenotypes observed in hypomorphic strains. Nevertheless, the fortuitous *dksA1* mutation allowed the opportunity to further explore the regulatory dynamics between DksA and PsrA. The bacterial response to LCFA suggests a novel regulatory link to the stringent response pathway, further solidifying the mechanistic importance of both DksA and PsrA as contributing regulators of the biphasic lifestyle of *L. pneumophila.*

In summary, PsrA seems to redundantly act as a bypass for *dksA* in virulence but has little impact on other processes, suggesting a more targeted mechanism. The largely overlapping and additive phenotypes presented in this study are consistent with the two distinct mechanisms by which DksA and PsrA act, and thus the following model is proposed (Figure 12). In a scenario in which a promoter that is repressed by either DksA or PsrA; absence of DksA would permit GreA to act as the sole-secondary channel binding protein thereby allowing increased

efficiency in transcription initiation. Elevated levels of PsrA would result in increased promoter blockage at co-regulated promoters, thus providing a compensatory repression. Conversely, lack of PsrA would leave the promoter more accessible for RNAP, but this could be counteracted if elevated levels of DksA results in reduced transcriptional efficiency. Alternatively, a promoter not subject to PsrA influence would be exempt from the compensatory effects, and thus be wholly dependent on the dynamics between GreA and DksA. Nevertheless, the proposed co-regulator duality could explain why transcriptomic analyses did not overtly reveal a large number of PsrA-regulated targets (Graham *et al*., 2021); thus, future transcriptomic studies will include the Δ*psrA* Δ*dksA* strain to compare against data obtained for individual Δ*psrA* and Δ*dksA* strains to discern distinct and overlapping roles.

Another major question is whether the observations garnered from the Δ*dksA* strain can be extended to include the ppGpp^0 (Δ*relA* Δ*spoT*) strain. The interface with PsrA and ppGpp remains unexplored and bears interest in relation to the link between PsrA and the fatty acid response. The possibility that PsrA is the mechanism by which DksA drives the LCFA response in ppGpp^0 strain is intriguing. Additionally, whether a similar reciprocal compensatory effect on phenotypes is seen between ppGpp^0 and PsrA poses an interesting topic for future investigation to follow upon the present study, which explored the phenotypic role of spontaneously mutated DksA1 and PsrA, and uncovered a synergistic genetic relationship between PsrA and DksA in terms of virulence regulation.

Acknowledgements

We thank M. Swanson (University of Michigan) for her kind gift of pBH6119 and Lp02, J. Vogel (Washington University) for his kind gift of pSR47s and pJB908, R. R. Isberg (Tufts University) for his kind gift of Lp03. This work was supported by Natural Sciences and Engineering Research Council (NSERC) Discovery Grant funds awarded to A.K.C.B (RGPIN-2019-05490), T.dK. (RPIN-2017-04970) and G.P. (RGPIN-2018-04968), and Canadian Foundation for Innovation (CFI) Grant funds to A.K.C.B. Research personnel were supported by University of Manitoba Faculty of Graduate Studies (C.G., T.M, T.P., J.B.), Research Manitoba Master's Studentship Award (T.P.), and NSERC CGS Masters (T.M, A.G.) and Doctoral (T.M., T.P, A.G.).

Experimental Procedures

Structural Predictions and Modelling The amino acid sequences of DksA and DskA1 were submitted to the collabfold2 sever (Pettersen *et al*. 2021) with default settings. Top rank #1 models were selected for modelling and analysis in UCSF ChimeraX (Pettersen *et al*., 2021). Structural overlays between Lp02 DksA, DksA1, and DksA (5VSW) (Molodtsov *et al*., 2018) were aligned with Matchmaker. Conservation alignments were performed using Consurf (Landau *et al*., 2005; Ashkenazy *et al*., 2016) with the Alphafold2 model of Lp02 DksA.

Culture of *E. coli* and *L pneumophila* *Legionella pneumophila* Philadelphia-1 derivative Lp02 parental and isogenic strains, as described in Table 1, were grown as previously described on Buffered-Charcoal-Yeast Extract BCYE)-agar plates (Feeley *et al.*, 1979) supplemented as required with thymidine (100 μg/mL), sucrose (5% w/v) or kanamycin sulphate (25 μg/mL) and incubated at 37°C and 5% CO_2, or Buffered-Yeast Extract (BYE) broth at 37°C. *E. coli* was utilized for cloning and plasmid propagation purposes (DH5α for *in trans* expression vector pJB908 or pThy [pBH6119], and DH5α λpir for suicide vector pSR47S)was grown on LB (Lennox) agar or broth supplemented as required with ampicillin (100 μg/mL) or kanamycin sulphate (40 μg/mL) and incubated at 37°C.

Molecular methods/reagents, cloning, and sequencing Chemicals were procured form VWR (Ottawa, ON, Canada), Thermo-Fisher (Mississauga, ON, Canada), or Sigma-Aldrich (Oakville, ON, Canada) while restriction enzymes, PCR enzymes, and other cloning reagents were procured from New England Biolabs (Whitby, ON, Canada). Oligonucleotide primers, ordered from Life Technologies (Thermo-Fisher), were utilized under conditions listed in Table 2.

Nucleic acid purification kits were purchased from Qiagen (Toronto, ON, Canada). Sanger sequencing for routine verification of constructs and mutant validations was done as a fee-based service by The Centre for Applied Genomics (The Hospital for Sick Children, Toronto, ON, Canada). Whole genome sequencing was undertaken by phenol-chloroform isolation of genomic DNA followed by sequencing via Pacbio SMRT at Genome-Québec (Montreal, QC, Canada) and assembled using Geneious™ software.

***dskA1* and Δ*dksA* mutant strains** The *dksA1* mutation was identified during routine whole genome sequencing of prospective Δ*psrA* mutant strains during experiments for Graham *et al.* (2021), and traced back to the electrocompetent cell stock used to create the strains, which was subsequently struck out for isolated colonies. Colonies were screened for *dksA1* by PCR using the primer set (PF dksA1 missing / PR dksA1 missing) that annealed to the missing 24 bp region within *dksA1*, allowing recovering of the ancestral Lp02 *dksA1* strain from the competent cells. For these reactions, PF dksA1 missing was paired with PR dksA ext conf, and PF dksA ext conf was paired with PR dksA1 missing, such that each primer set only generated product from the parental allele. As a positive PCR control, adjacent PF/PR dksA conf int primer set generated product in both alleles. For generation of an in-frame Δ*dksA* mutant strain, ~1000 bp 5′ (primer set PF 5-flk dksA SalI / PR 5-flk dksA BamH1) and 3′ (PF 3-flk dksA BamH1 / PR 3-flk dksA SacI) regions flanking *dksA* were PCR-amplified and cloned into suicide vector pSR47S to use for routine allelic exchange. For generation of *in trans* complementation or overexpression constructs, either *dksA* or *dksA1* were PCR-amplified from Lp02 or *dksA1* mutant CG799, respectively, using primer set (PF comp dksA BamHI / PR comp dksA SacI) and cloned into pJB908, and introduced into parental or isogenic mutant strains by electroporation. Plasmid

constructs and mutations were routinely verified by sequencing isolated plasmids or PCR amplicon products, and mutant strains were routinely subjected to whole genome sequencing to rule out secondary mutations.

***In vitro* growth kinetics** *L. pneumophila* strains were streaked on BCYE and grown for three days under standard conditions. Bacterial cell mass was collected with a disposable loop and suspended in pre-warmed BYE broth and normalized to OD_{600} = 0.15 in BYE broth. Subsequently 150 µL of this suspension was loaded in triplicate wells in a 96-well flat bottomed microtitre plate, the lid was sealed with Parafilm, and loaded into a BioTek Synergy HTX plate reader, reading OD_{600} hourly for 24 h at 37°C or every 2 h for 48 h at 25°C with 150 rpm linear shaking. Results were plotted in GraphPad Prism™ 9.1 and analyzed via two-way ANOVA analysis.

Culture and intracellular kinetics in protozoan *A. castellanii* *Acanthamoeba castellanii* (ATCC 30234) were propagated in PYG media at 25°C as previously described (Tanner *et al.*, 2016). Briefly, infections were undertaken in AC buffer by placing ~10^6 protozoan trophozoites in each well of a set of 24 tissue culture-treated 24-well plates and allowing them to adhere, then overlaying them with bacteria normalized by OD_{600} to a MOI of 0.1 in AC buffer. After 1 h incubation at 25°C, the wells were washed 3 x 1 mL AC buffer, before incubating in 1 mL/well of AC buffer at 25°C until the indicated timepoints. Protozoa were lysed mechanically via vortexing, and the lysate serially diluted in AC buffer onto BCYE-agar plates to enumerate titres. To enhance enumeration of difficult-to-recover avirulent strains, a portion of the lysate was tenfold concentrated by centrifugation at 21,000 x *g* in a microcentrifuge for 2 min, then 0.9 vol

of the supernatant drawn off; the pellet was resuspended in the remaining volume and spotted alongside the serial dilutions. After counting titres, graphs were plotted and analyzed (two-way ANOVA) in GraphPad Prism™ 9.1.

Culture and intracellular kinetics in U937 human macrophages Human U937 monocytic cells were propagated and differentiated into macrophages using phorbol myristate acetate (PMA, Sigma-Aldrich) as previously described (Tanner *et al.*, 2016). Cells were grown in RPMI-1640 media (HyClone, Thermo-Fisher) supplemented with 10% heat inactivated fetal bovine serum (Seradigm, Mississauga, ON) (RPMI + FBS) at 37°C and 5% CO_2 that was used for all washes and incubations in a pre-warmed state. For infection, ~ 10^6 activated U937-derived macrophages were placed into each well of a tissue culture-treated 24 well plates, allowed to adhere, and overlaid with *L. pneumophila* strains normalized by OD_{600} to a MOI of 2, for 1 h. The bacteria were washed away with 3 x 1 ml washes in RPMI + FBS, followed by an incubation for 1 h with RPMI + FBS with 100 µg/mL gentamicin. After a further 3 x 1 mL washes in RPMI + FBS, the cells were incubated in 1 mL RPMI + FBS until lysis at indicated timepoints. Cells were lysed osmotically by replacing the RPMI + FBS with ice-cold HyClone ultrapure water and repeated pipetting (Thermo-Fisher), then serially diluting the lysate in additional HyClone water and enumerating *L. pneumophila* titres by spotting the dilutions on BCYE-agar plates. After counting, graphs were plotted and analyzed via two-way ANOVA in GraphPad Prism™ 9.1.

Pigment, morphology and capturability assays Suspensions of *L. pneumophila* were prepared as per *in vitro* growth kinetics. Pigment assays were undertaken in accordance to Wiater et al.

(1994). Briefly, inoculated 5 mL BYE broth cultures in 13 mL plastic test tubes were placed on a roller drum at 37°C for 72 h. To quantify pigment at 24 h timepoints, 1 mL of culture was withdrawn, pelleted at 21,000 x g in a microcentrifuge for 2 min, after which 150 µL of supernatant was loaded in triplicate into 96 well plates and read for absorbance at 550 nm on a BioTek Synergy HTX plate reader (Wiater *et al*., 1994). After removal of residual supernatant, the pellet was suspended in 1 mL of 1 x PBS pH 7.0 and similarly loaded (150 µL) into a 96 well plate then read for OD_{600}. Blank controls were the same volume of BYE or 1 x PBS as appropriate. Results were plotted and analyzed using GraphPad Prism™ (9.1). Photographed samples were prepared similarly and at specified allowed to sit undisturbed for 24 h at ambient temperatures (~22°C) for cells to sediment out by gravity. Long-term culturability was assessed by inoculating 96 well plates with six wells for each strain, containing 150 µL of an OD_{600} = 0.15 suspension in BYE. The outermost rows and columns were filled with sterile water to reduce evaporation, the plates were sealed with Parafilm and incubated on a shaking platform at 37°C for four days. At indicated intervals, cell aggregates were dispersed with pipetting, the OD_{600} was read with a BioTek Synergy HTX plate reader across the wells containing unharvested culture, and one well of each strain harvested and serially diluted for titre on BCYE agar plates. Results were plotted and analyzed using GraphPad Prism (9.1). For colony-spot morphology, 10 µL of the residual OD_{600} = 0.15 suspension used to prepare these assays was spotted on a BCYE plate with spots spread out to twice the spacing of a standard multi-channel pipette then incubated for 4 days at 37ºC and 5% CO_2, then photographed.

LCFA assays Suspensions of *L. pneumophila* strains were prepared as per the *in vitro* kinetics, at OD_{600} = 0.15 in BYE broth, except that media was supplemented with two-fold serially diluted

concentrations of palmitic acid (PA) as a 40 mM stock dissolved in 100% ethanol. All broth including PA dilutions, controls and blanks was normalized to 0.5% ethanol. The suspension was then subject to a standard in vitro growth curve as described in the in vitro kinetics section. Inhibition was defined as growth of <50% in comparison to that of the same strain in a BYE + 0.5% ethanol-only control at the end of 24 h. Data were graphed using GraphPad Prism™ 9.1.

Microscopy Microscopy and cell lengths were conducted as per Graham *et al.*, (2021). Briefly, broth cultures in BYE broth were inoculated at OD_{600} = ~0.02 and incubated for 18 hto OD_{600} = 0.5-1.0 at 37°C to enter exponential phase, then were mounted on a 2% w/v agarose pad prepared in water and imaged on an Axio Observer Z1 inverted microscope (Zeiss) equipped with a glycerol-immersion 150X objective. Stationary phase cells were imaged by returning the cultures to the roller drum for a further ~24 h to achieve stationary phase and imaged similarly. Cell lengths were quantified using the length tool in ImageJ and lengths plotted and analyzed in GraphPad Prism™ (9.1).

Table 1 List of strains and plasmids

Number	Name	Description	Source/reference
E. coli			
	DH5α	F′ *endA1 hsdR17*(r_k- m_k-) *supE44 thi-1 recA1 gyrA* (*Nal*^{r}) *relA1* Δ(*lacZYA-argF*)*U169 deoR*(ϕ80lacΔ(lacZ)M15)	New England Biolabs
	DH5α λpir	K-12 F- φ80*lacZ*ΔM15 *endA recAhsdR17* (*rm-mK+*) *supE44 thi-1 gyrA96 relA1* Δ(*lacZYA-argF*) U169 *λpir*	M. Swanson (Bryan *et al*., 2013)
L. pneumophila			
C858	Lp02	Str^r, Thy$^-$, HsdR$^-$ derivative of Philadelphia-1 strain	M. Swanson (Berger and Isberg, 1993)
KB265	Lp03	Lp02 Δ*dotA* mutant	R. Isberg (Berger and Isberg, 1993)
CG859	Δ*psrA*	Lp02 Δ*psrA* (unmarked, in frame deletion mutant)	Graham *et al.*, (2021)
CG860	Lp02 pThy	Lp02 pBH6119	Tanner *et al.*, (2016)
JT708	Δ*dotA* pThy	Lp03 pBH6119	Tanner *et al.*, (2016)
CG861	Lp02 pComp-*psrA*	Lp02 pJB908-*psrA*	Graham *et al.*, (2021)
CG862	Δ*psrA pThy*	Δ*psrA* pThy	Graham *et al.*, (2021)
CG863	Δ*psrA* pComp-*psrA*	Δ*psrA* pJB908-*psrA*	Graham *et al.*, (2021)
CG799	*dksA1*	Lp02 *dksA1* (*dksA1*[Δ*170-194]*); spontaneous 24 bp in-frame deletion	This study
CG819	*dksA1* pThy	*dksA1* pBH6119	This study
CG813	*dksA1*Δ*psrA*	Lp02 *dksA1* Δ*psrA*	This study
CG826	*dksA1* Δ*psrA* pThy	*dksA1* Δ*psrA* pBH6119	This study
CG1053	Δ*dksA*	Lp02 Δ*dksA* (unmarked, in frame deletion mutant of *dksA*)	This study
CG1054	Δ*dksA* Δ*psrA*	Δ*psrA* Δ*dksA*	This study
CG1055	Δ*dksA* pThy	Δ*dksA* pBH6119	This study
CG1056	Δ*dksA* Δ*psrA* pThy	Δ*psrA* Δ*dksA* pBH6119	This study
CG1057	Δ*dksA* pComp-*dksA*	Δ*dksA* pBH6119	This study
CG1059	Lp02 pComp-*dksA*	Lp02 pJB908-*dksA*	This study
CG1060	Δ*psrA* pComp-*dksA*	Δ*psrA* pJB908-*dksA*	This study
CG1061	Δ*dksA* pComp-*psrA*	Δ*dksA* pJB908-*psrA*	This study
CG1101	Δ*dksA* pComp-*dksA1*	Δ*dksA* pJB908-*dksA1*	This study
CG1102	Lp02 pComp-*dksA1*	Lp02 pComp-*dksA1*	This study
CG1146	*dksA1* pComp-*dksA*	*dksA1* pComp-*dksA*	This study
Plasmids			
	pJB908	RSF1010 cloning vector, *td*Δ*i*, Amp^r Thy$^+$	J. Vogel (Sexton *et al*., 2004)
	pBH6119	RSF1010 promoterless GFP vector; Amp^r, Thy$^+$	M. Swanson (Hammer *et al*., 2002)
	pSR47S	oriTRP4 oriR6K *kan*^{r} *sacB*	J. Vogel (Merriam *et al*., 1997)
pPP619	pComp-*psrA*	pJB908-*psrA*	Graham *et al.*, (2021)

pCG1051	pComp-*dksA*	pJB908-*dksA*	This study
pCG1080	pComp-*dksA1*	pJB908-*dksA1* allele recovered from spontaneous *dksA1* Lp02 strain CG799	This study
pCG1069	pSR47S-5′flk-*ΔdksA*-3′flk	pSR47S with 5′ and 3′ flanking regions for Δ*dksA*	This study

Table 2 List of oligonucleotides.

Name	Sequence	Annealing Temp. (ºC)	Product Size (bp)
Cloning/Confirmation			
PF 5-flk dksA SalI	gcgataGTCGACgttagaggcagaacttttactctg	62	915
PR 5-flk dksA BamH1	gcgataGGATCCatcaattaattgtcctgtcatgcc		
PF 3-flk dksA BamH1	gcgataGGATCCcagggtgcttgattctttcttg	62	978
PR 3-flk dksA SacI	gcgataGAGCTCgtaataagggctctgtagtgagg		
PF comp dksA BamHI	gcgataGGATCCgatttcagcaaagaggcattgg	62	1016 (*dksA*) 992 (*dksA1*)
PR comp dksA SacI	gcgataGAGCTCgaatcaagcaccctgattttgg		
PF dksA ext conf	caagcaatcggaataacaaacc	62	842
PR dksA ext conf	cactgtaagccttgttgattttc		
PR dksA conf int	gtcttgcttcaagacgtttcag	57.5	533 (with PF ext dksA conf)
pF dksA1 missing*	ggaagaagtagatcgtactgtctc	57.5	320 with pF ext dksA conf*
PR dksA1 missing*	gagacagtacgatctacttcttcc	57.5	546 to pR ext dksA conf*
Sequencing			
PF pSR47s seq	ctgttgcatgggcataaagttg	-	–
PR pSR47s seq	cacaggaaacagctatgacc	-	-
PF pJB908 seq	ctccgtgatggaatgacaac	-	–
PR pJB908 seq	gaccgcttctgcgttctga	-	–

Restriction sites indicated by capitalized letters.

* dksA1 missing primers used for screening strains, anneal to the region missing in *dksA1* and will only generate product with the parental allele.

References

1. Abdelhady, H. and Garduño, R.A. (2013) The progeny of *Legionella pneumophila* in human macrophages shows unique developmental traits. *FEMS Microbiol Lett*. **349**:99-107.
2. Aberg, A., Shingler, V. and Balsalobre, C. (2008) Regulation of the *fimB* promoter: a case of differential regulation by ppGpp and DksA *in vivo*. *Mol Microbiol*. **67**:1223-1241.
3. Aberg, A., Fernández-Vázquez, J., Cabrer-Panes, J.D., Sánchez, A. and Balsalobre, C. (2009). Similar and divergent effects of ppGpp and DksA deficiencies on transcription in *Escherichia coli. J Bacteriol.* **191**: 3226-3236.
4. Abu-Zant, A., Asare, R., Graham, J.E. and Abu Kwaik, Y. (2006. Role for RpoS but not RelA of *Legionella pneumophila* in modulation of phagosome biogenesis and adaptation to the phagosomal microenvironment. *Infect Immun.* **74**:3021-3026.
5. Al-Khodor, S., Kalachikov, S., Morozova, I., Price, C. T. and Abu Kwaik, Y. (2009) The PmrA/PmrB two-component system of *Legionella pneumophila* is a global regulator required for intracellular replication within macrophages and protozoa. *Infect Immun*. **77**:374-386.
6. Anderson, S.E., Vadia, S.E., McKelvy, J. and Levin, P.A. (2023) The transcription factor DksA exerts opposing effects on cell division depending on the presence of ppGpp. *mBio* **14**(6):e0242523.
7. Ashkenazy, H., Abadi, S., Martz, E., Chay, O., Mayrose, I., Pupko, T. and Ben-Tal, N. (2016) ConSurf 2016: an improved methodology to estimate and visualize evolutionary conservation in macromolecules. *Nucleic Acids Res* 8;**44**(W1):W344-50.
8. Bachman, M.A. and Swanson**,** M.S. (2001) RpoS co-operates with other factors to induce *Legionella pneumophila* virulence in the stationary phase. *Mol Microbiol.* **40**:1201-1214.

9. Burstein, D., Amaro, F., Zusman, T., Lifshitz, Z., Cohen, O., Gilbert, J.A., Pupko, T., Shuman, H.A. and Segal, G. (2016) Genomic analysis of 38 *Legionella* species identifies large and diverse effector repertoires. *Nat Genet.* **48**:167-175.
10. Chatfield, C.H. and Cianciotto, N.P. (2007). The secreted pyomelanin pigment of *Legionella pneumophila* confers ferric reductase activity. *Infect Immun*. **75**: 4062-4070.
11. Chatterji, D., Fujita, N. and Ishihama, A. (1998) The mediator for stringent control, ppGpp, binds to the beta-subunit of *Escherichia coli* RNA polymerase. *Genes Cells* **3**:279-287.
12. Dalebroux, Z.D., Yagi, B.F., Sahr, T., Buchrieser, C. and Swanson, M.S. (2010) Distinct roles of ppGpp and DksA in *Legionella pneumophila* differentiation. *Mol Microbiol.* **6**:200-219.
13. Edwards, R.L., Dalebroux, Z.D. and Swanson, M.S. (2009) *Legionella pneumophila* couples fatty acid flux to microbial differentiation and virulence. *Mol Microbiol.* **71**:1190-1204.
14. Faulkner, G. and Garduño, R.A. (2002) Ultrastructural analysis of differentiation in *Legionella pneumophila. J Bacteriol.* **184**:7025-7041.
15. Feldheim Y.S., Zusman T., Speiser Y. and Segal G. (2016) The *Legionella pneumophila* CpxRA two-component regulatory system: new insights into CpxR's function as a dual regulator and its connection to the effectors regulatory network. *Mol Microbiol.* **99**:1059-1079.
16. Finsel, I. and Hilbi, H. (2015) Formation of a pathogen vacuole according to *Legionella pneumophila*: how to kill one bird with many stones. *Cell Microbiol*. **17**:935-950.
17. Fonseca, M.V. and Swanson, M.S. (2014) Nutrient salvaging and metabolism by the intracellular pathogen *Legionella pneumophila*. *Front Cell Infect Microbiol.* **4**:12.

18. Garduño, R.A., Garduño, E., Hiltz, M. and Hoffman, P.S. (2002) Intracellular growth of *Legionella pneumophila* gives rise to a differentiated form dissimilar to stationary-phase forms. *Infect Immun.* **70**:6273-6283.

19. Gomez-Valero, L., Rusniok, C., Carson, D., Mondino, S., Pérez-Cobas, A.E., Rolando, M., Pasricha, S., Reuter, S., Demirtas, J., Crumbach, J., Descorps-Declere, S., Hartland, E.L., Jarraud, S., Dougan, G., Schroeder, G.N., Frankel, G. and Buchrieser, C. (2019) More than 18,000 effectors in the *Legionella* genus genome provide multiple, independent combinations for replication in human cells. *Proc Natl Acad Sci U S A.* **116**:2265-2273.

20. Gourse, R.L., Chen, A.Y., Gopalkrishnan, S., Sanchez-Vazquez, P., Myers, A. and Ross, W. (2018) Transcriptional Responses to ppGpp and DksA. *Annu Rev Microbiol.* **72**:163-184.

21. Graham, C.I., Patel, P.G., Tanner, J.R., Hellinga, J., MacMartin, T.L., Hausner, G. and Brassinga, A.K.C. (2021) Autorepressor PsrA is required for optimal *Legionella pneumophila* growth in *Acanthamoeba castellanii* protozoa. *Mol Microbiol*. **116**:624-647.

22. Graham, C.I., MacMartin, T.L., de Kievit, T.R. and Brassinga, A.K.C. (2024) Molecular regulation of virulence in *Legionella pneumophila*. *Mol Microbiol*. **121**:167-195.

23. Gummesson, B., Lovmar, M. and Nyström, T. (2013) A proximal promoter element required for positive transcriptional control by guanosine tetraphosphate and DksA protein during the stringent response. *J Biol Chem.* **288**:21055–21064.

24. Hales, L.M. and Shuman, H.A. (1999) The *Legionella pneumophila rpoS* gene is required for growth *within Acanthamoeba castellanii*. *J Bacteriol.* **181**:4879-4889.

25. Hammer, B.K., Tateda, E.S. and Swanson, M.S. (2002) A two-component regulator induces the transmission phenotype of stationary-phase *Legionella pneumophila. Mol Microbiol.* **44**:107-118.

26. Häuslein, I., Sahr, T., Escoll, P., Klausner, N., Eisenreich, W. and Buchrieser, C. (2017) *Legionella pneumophila* CsrA regulates a metabolic switch from amino acid to glycerolipid metabolism. *Open Biology* **7**:170149.

27. Hovel-Miner, G., Pampou, S., Faucher, S.P., Clarke, M., Morozova, I., Morozov, P., Russo, J.J., Shuman, H.A. and Kalachikov, S. (2009) SigmaS controls multiple pathways associated with intracellular multiplication of *Legionella pneumophila. J Bacteriol.* **191**:2461-2473.

28. Isberg, R.R., O'Connor, T.J. and Heidtman, M. (2009) The *Legionella pneumophila* replication vacuole: making a cozy niche inside host cells. *Nat Rev Microbiol.* **7**:13-24.

29. Jumper, J., Evans, R., Pritzel, A., Green, T., Figurnov, M., Ronneberger, O., Tunyasuvunakool, K., Bates, R., Žídek, A., Potapenko, A., Bridgland, A., Meyer, C., Kohl, S.A.A., Ballard, A.J., Cowie, A., Romera-Paredes, B., Nikolov, S., Jain, R., Adler, J., Back, T., Petersen, S., Reiman, D., Clancy, E., Zielinski, M., Steinegger, M., Pacholska, M., Berghammer, T., Bodenstein, S., Silver, D., Vinyals, O., Senior, A.W., Kavukcuoglu, K., Kohli, P. and Hassabis, D. (2021) Highly accurate protein structure prediction with AlphaFold. *Nature* **596**(7873):583-589.

30. Kagan, J.C. and Roy, C.R. (2002) *Legionella* phagosomes intercept vesicular traffic from endoplasmic reticulum exit sites. *Nat Cell Biol.* **4**:945-954.

31. Kang, Y., Nguyen, D.T., Son, M.S. and Hoang, T.T. (2008) The *Pseudomonas aeruginosa* PsrA responds to long-chain fatty acid signals to regulate the *fadBA5* beta-oxidation operon. *Microbiology* **154**:1584-1598.

32. Landau, M., Mayrose, I., Rosenberg, Y., Glaser, F., Martz, E., Pupko, T. and Ben-Tal, N. (2005) ConSurf 2005: the projection of evolutionary conservation scores of residues on protein structures. *Nucleic Acids Res* **33**(Web Server issue):W299-302.

33. Lemke, J.J., Sanchez-Vazquez, P., Burgos, H.L., Hedberg, G., Ross, W. and Gourse, R.L. Direct regulation of *Escherichia coli* ribosomal protein promoters by the transcription factors ppGpp and DksA. *Proc Natl Acad Sci USA.* **108**(14):5712-7.

34. Levin, T.C., Goldspiel, B.P., Malik, H.S. (2019). Density-dependent resistance protects *Legionella pneumophila* from its own antimicrobial metabolite, HGA. *Elife.* **8**: e46086.

35. McNealy, T.L., Forsbach-Birk, V., Shi, C. and Marre, R. (2005) The Hfq homolog in *Legionella pneumophila* demonstrates regulation by LetA and RpoS and interacts with the global regulator CsrA. *J Bacteriol.* **187**:1527-1532.

36. Magnusson, L.U., Gummesson, B., Joksimović, P., Farewell, A. and Nyström, T. (2007) Identical, independent, and opposing roles of ppGpp and DksA in *Escherichia coli. J Bacteriol.* **189**:5193-5202.

37. Molodtsov, V., Sineva, E., Zhang, L., Huang, X., Cashel, M., Ades, S.E. and Murakami, K.S. (2018) Allosteric Effector ppGpp Potentiates the Inhibition of Transcript Initiation by DksA. *Mol Cell* **69**(5):828-839.e5.

38. Molofsky, A.B. and Swanson, M.S. (2004) Differentiate to thrive: lessons from the *Legionella pneumophila* life cycle. *Mol Microbiol.* **53**:29-40.

39. Mondino, S., Schmidt, S. and Buchrieser, C. (2020) Molecular mimicry: a paradigm of host-microbe coevolution illustrated by *Legionella*. *mBio* **11**:e01201-20.

40. Morash, M.G., Brassinga, A.K., Warthan, M., Gourabathini, P., Garduño, R.A., Goodman, S.D. and Hoffman, P.S. (2009) Reciprocal expression of integration host factor and HU in the developmental cycle and infectivity of *Legionella pneumophila*. *Appl Environ Microbiol.* **75**:1826-1837.

41. Myers, A.R., Thistle, D.P., Ross, W. and Gourse, R.L. (2020) Guanosine Tetraphosphate Has a Similar Affinity for Each of Its Two Binding Sites on *Escherichia coli* RNA Polymerase. *Front Microbiol* **11**:587098.

42. Nevo, O., Zusman, T., Rasis, M., Lifshitz, Z. and Segal, G. (2014) Identification of *Legionella pneumophila* effectors regulated by the LetAS-RsmYZ-CsrA regulatory cascade, many of which modulate vesicular trafficking. *J Bacteriol.* **196**:681-692.

43. Newton, H.J., Ang, D.K., van Driel, I.R. and Hartland, E.L. (2010) Molecular pathogenesis of infections caused by *Legionella pneumophila. Clin Microbiol Rev.* **23**:274-298.

44. Oliva, G., Sahr, T. and Buchrieser, C. (2018) The life cycle of *L. pneumophila*: cellular differentiation is linked to virulence and metabolism. *Front Cell Infect Microbiol.* **8**:3.

45. Parshin, A., Shiver, A.L., Lee, J., Ozerova, M., Schneidman-Duhovny, D., Gross, C.A. and Borukhov, S. (2015) DksA regulates RNA polymerase in *Escherichia coli* through a network of interactions in the secondary channel that includes Sequence Insertion 1. *Proc Natl Acad Sci U S A* **112**(50):E6862-71.

46. Perederina, A., Svetlov, A., Vassylyeva, M., Tahirov, T., Yokoyama, S., Artsimovitch, I. and Vassylyev, D. (2004). Regulation through the secondary channel-structural framework for ppGpp-DksA synergism during transcription. *Cell* **118**:297-309.

47. Personnic, N., Striednig, B. and Hilbi, H. (2018) *Legionella* quorum sensing and its role in pathogen-host interactions. *Curr Opin Microbiol.* **41**:29-35.

48. Pettersen, E.F., Goddard, T.D., Huang, C.C., Meng, E.C., Couch, G.S., Croll, T.I., Morris, J.H. and Ferrin, T.E. (2021) UCSF ChimeraX: Structure visualization for researchers, educators, and developers. *Protein Sci.* **30**(1):70-82.

49. Pitre, C.A.J., Tanner, J.R., Patel, P. and Brassinga, A.K.C. (2013) Regulatory control of temporally expressed integration host factor (IHF) in *Legionella pneumophila. Microbiology* **159**:475-492.

50. Potrykus, K. and Cashel, M. (2008) (p)ppGpp: still magical? *Annu Rev Microbiol*. **62**:35-51.

51. Rasis, M. and Segal, G. (2009) The LetA-RsmYZ-CsrA regulatory cascade, together with RpoS and PmrA, post-transcriptionally regulates stationary phase activation of *Legionella pneumophila* Icm/Dot effectors. *Mol Microbiol.* **72**:995-1010.

52. Robertson, P., Abdelhady, H. and Garduño, R.A. (2014) The many forms of a pleomorphic bacterial pathogen-the developmental network of *Legionella pneumophila*. *Front Microbiol*. **5**:670.

53. Ross, W., Vrentas, C.E., Sanchez-Vazquez, P., Gaal, T. and Gourse, R.L. (2013) The magic spot: a ppGpp binding site on *E. coli* RNA polymerase responsible for regulation of transcription initiation. *Mol Cell* **50**(3):420-9.

54. Ross, W., Sanchez-Vazquez, P., Chen, A.Y., Lee, J.H., Burgos, H.L. and Gourse, R.L. (2016) ppGpp Binding to a Site at the RNAP-DksA Interface Accounts for Its Dramatic Effects on Transcription Initiation during the Stringent Response. *Mol Cell* **62**(6):811-823.

55. Rowbotham, T.J. (1986) Current views on the relationships between amoebae, legionellae and man. *Isr J Med Sci*. **22**:678-689.

56. Sahr, T., Bruggemann, H., Jules, M., Lomma, M., Albert-Weissenberger, C., Cazalet, C. and Buchrieser, C. (2009) Two small ncRNAs jointly govern virulence and transmission in *Legionella pneumophila. Mol Microbiol.* **72**:741-762.

57. Sahr, T., Rusniok, C., Dervins-Ravault, D. Sismeiro, O., Coppée, J.Y. and Buchrieser, C. (2012) Deep sequencing defines the transcriptional map of *L. pneumophila* and identifies growth phase-dependent regulated ncRNAs implicated in virulence. *RNA Biol*. **9**:503-19.

58. Sahr, T., Rusniok, C., Impens, F., Oliva, G., Sismeiro, O., Coppée, J.Y. and Buchrieser, C. (2017) The *Legionella pneumophila* genome evolved to accommodate multiple regulatory mechanisms controlled by the CsrA-system. *PLoS Genet.* **13**:e1006629.

59. Schell, U., Kessler, A. and Hilbi, H. (2014) Phosphorylation signalling through the *Legionella* quorum sensing histidine kinases LqsS and LqsT converges on the response regulator LqsR. *Mol Microbiol.* **92**:1039-1055.

60. Skolnick, J., Gao, M., Zhou, H. and Singh, S. (2021) AlphaFold 2: Why It Works and Its Implications for Understanding the Relationships of Protein Sequence, Structure, and Function. *J Chem Inf Model* **61**(10):4827-4831.

61. Steinert, M., Engelhard, H., Flugel, M., Wintermeyer, E. and Hacker J. (1995). The Lly protein protects *Legionella pneumophila* from light but does not directly influence its intracellular survival in *Hartmannella vermiformis*. *Appl Environ Microbiol.* **61**: 2428-2430.

62. Steinert, M., Hentschel, U. and Hacker, J. (2002) *Legionella pneumophila*: an aquatic microbe goes astray. *FEMS Microbiol Rev*. **26**:149-162.

63. Tanner, J.R., Li, L., Faucher, S.P. and Brassinga, A.K. (2016) The CpxRA two-component system contributes to *Legionella pneumophila* virulence. *Mol Microbiol.* **100**:1017-1038.

64. Tanner, J.R., Patel, P.G., Hellinga, J.R., Donald, L.J., Jimenez, C., LeBlanc, J.J. and Brassinga, A.K.C. (2017) *Legionella pneumophila* OxyR Is a redundant transcriptional regulator that contributes to expression control of the two-component CpxRA system. *J Bacteriol.* **199**:e00690-16.

65. Tiaden, A., Spirig, T., Weber, S.S., Brüggemann, H., Bosshard, R., Buchrieser, C. and Hilbi, H. (2007) The *Legionella pneumophila* response regulator LqsR promotes host cell interactions as an element of the virulence regulatory network controlled by RpoS and LetA. *Cell Microbiol.* **9**:2903-2920.

66. Tiaden, A., Spirig, T., Carranza, P., Brüggemann, H., Riedel, K., Eberl, L., Buchrieser, C. and Hilbi, H. (2008) Synergistic contribution of the *Legionella pneumophila lqs* genes to pathogen-host interactions. *J Bacteriol.* **190**:7532-7547.

67. Tilney, L.G., Harb, O.S., Connelly, P.S., Robinson, C.G. and Roy, C.R. (2001) How the parasitic bacterium *Legionella pneumophila* modifies its phagosome and transforms it into rough ER: implications for conversion of plasma membrane to the ER membrane. *J Cell Sci.* **114**:4637-4650.

68. Travis, B.A. and Schumacher, M.A. (2022) Diverse molecular mechanisms of transcription regulation by the bacterial alarmone ppGpp. *Mol Microbiol* **117**(2):252-260.

69. Vinella, D., Potrykus, K., Murphy, H. and Cashel, M. (2012) Effects on growth by changes of the balance between GreA, GreB, and DksA suggest mutual competition and functional redundancy in *Escherichia coli. J Bacteriol.* **194**:261–273.

70. Wiater, L.A., Sadosky, A.B. and Shuman, H.A. (1994) Mutagenesis of *Legionella pneumophila* using Tn*903* dll*lacZ*: identification of a growth-phase-regulated pigmentation gene. *Mol Microbiol*. **11**:641-653.

71. Zusman, T., Gal-Mor, O. and Segal, G. (2002) Characterization of a *Legionella pneumophila relA* insertion mutant and toles of RelA and RpoS in virulence gene expression. *J Bacteriol.* **184**:67-75.

72. Zusman, T., Aloni, G., Halperin, E., Kotzer, H., Degtyar, E., Feldman, M., Segal, G. (2007) The response regulator PmrA is a major regulator of the *icm/dot* Type IV secretion system in *Legionella pneumophila* and *Coxiella burnetii*. *Mol Microbiol.* **63**:1508-1523.

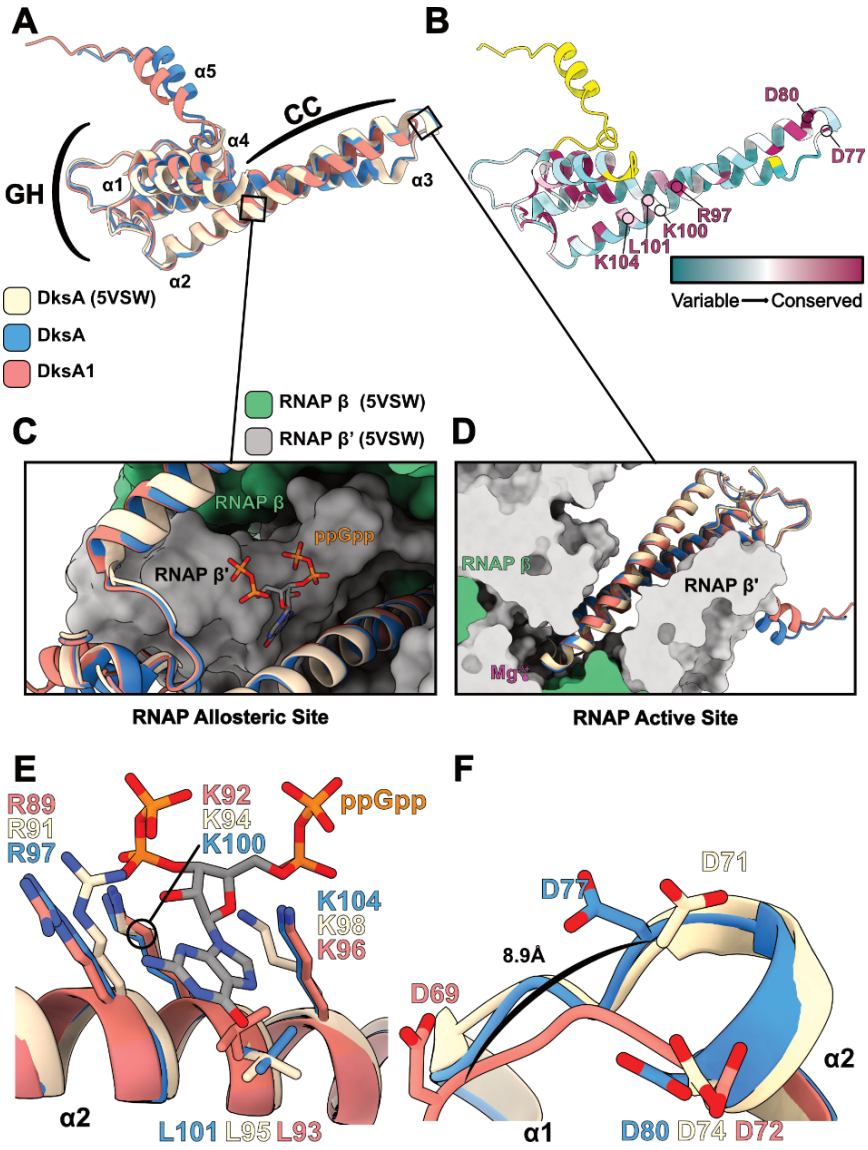

Figure 1: Structural comparison of DksA and DksA1 AlphaFold models. (A) Structural overlay of DksA (PDB ID: 5VSW) with both Lp02 DksA and DksA1 as modeled by AlphaFold. (B) Residue conservation of Lp02 DskA as plotted by the server Consurf (Landau *et al*., 2005; Ashkenazy *et al*., 2016). Yellow indicates insufficient information in the multisequence alignment. Indicated on the structure are conserved residues important for binding ppGpp and allostery with RNAP (R97 to K104), in addition to contact with the active site (D77-D80). (C) Binding of DksA with the RNAP allosteric site. A DksA:RNAP experimental structure (PDB ID: 5VSW) and aligned AlphaFold models are shown as cartoons, whereas RNAP is drawn as a molecular surface. The structure of ppGpp bound in the complex is also shown. (D) Slice view of DksA showing the contact point of residues D80 and D77 with magnesium in the RNAP active site. (D) Interactions of DksA variants with ppGpp in the RNAP allosteric site are shown and not disturbed by the truncation in DksA1. (E) Interactions of DksA variants with magnesium in the active site of RNAP are shown. AlphaFold predicts the truncation in DksA1 drastically moves the position of a critical aspartate residue (D69/71/77).

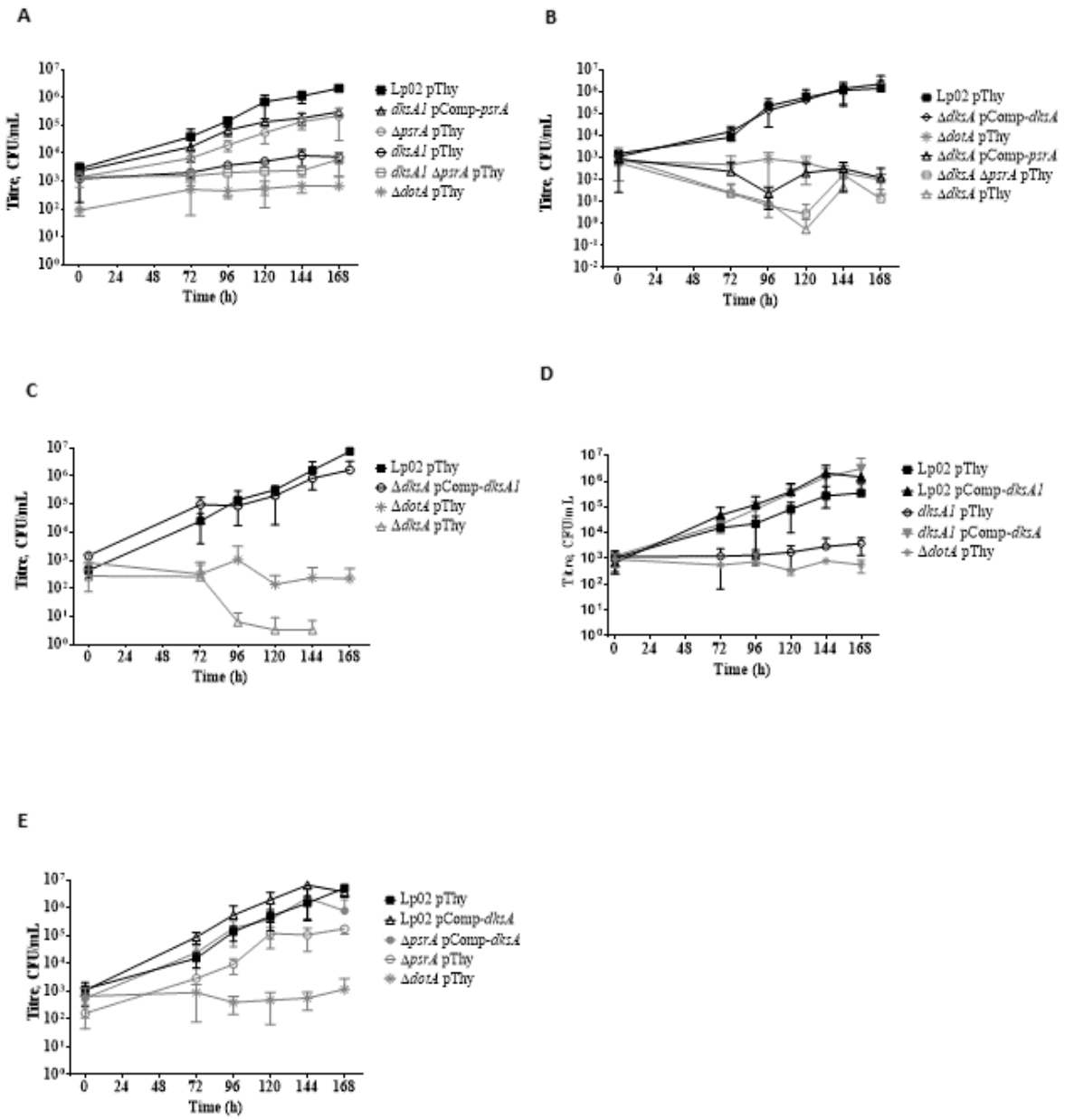

Figure 2: Synergistic impacts of DksA, DksA1, and PsrA on virulence of *L. pneumophila* in the *A. castellanii* protozoa. Intracellular growth kinetics of *L. pneumophila* strains in *A. castellanii* protozoa at 25ºC. Strains tested were parental Lp02 and isogenic strains featuring single or combinatorial genetics mutations (Δ*psrA*, Δ*dksA*, *dksA1*), *in-trans* complementation or overexpression of *psrA*, *dksA* or *dksA1* genes. Lp02 and Δ*dotA* are virulent (parental) and avirulent strains, respectively. Complementation/overexpression was via *in trans* plasmid expression with gene and endogenous promoter cloned into pJB908. pThy is empty control vector pBH6119. Error bars represent SD across mean of three biological replicates, with two technical replicates each. Samples below detection limit (~10 CFU/mL) were recorded as zero and omitted from graph if they lacked countable colonies across all replicates.

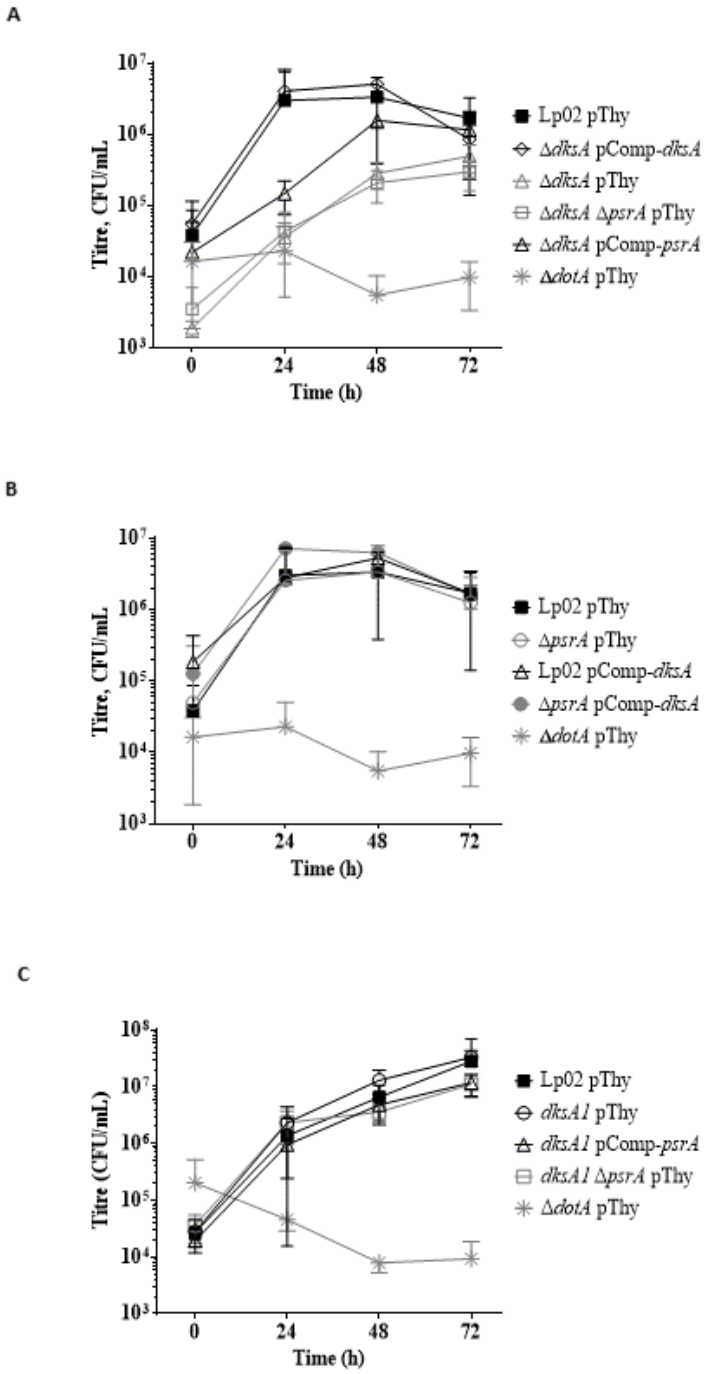

Figure 3: DksA is dispensable for growth in human macrophages. Intracellular growth kinetics of *L. pneumophila* strains in U937-derived macrophages at 37°C. Strains tested were parental Lp02 and isogenic strains featuring single or combinatorial genetic mutations (Δ*psrA*, Δ*dksA*, *dksA1*), *in-trans* complementation or overexpression of *psrA*, *dksA* or *dksA1* with gene and endogenous promoter cloned into pJB908. Lp02 and Δ*dotA* are virulent (parental) and avirulent strains, respectively. pThy is empty control vector pBH6119. Error bars represent SD across mean of three biological experiments with two technical replicates each. Experiments in panels A and B were conducted concurrently, but presented separately for clarity.

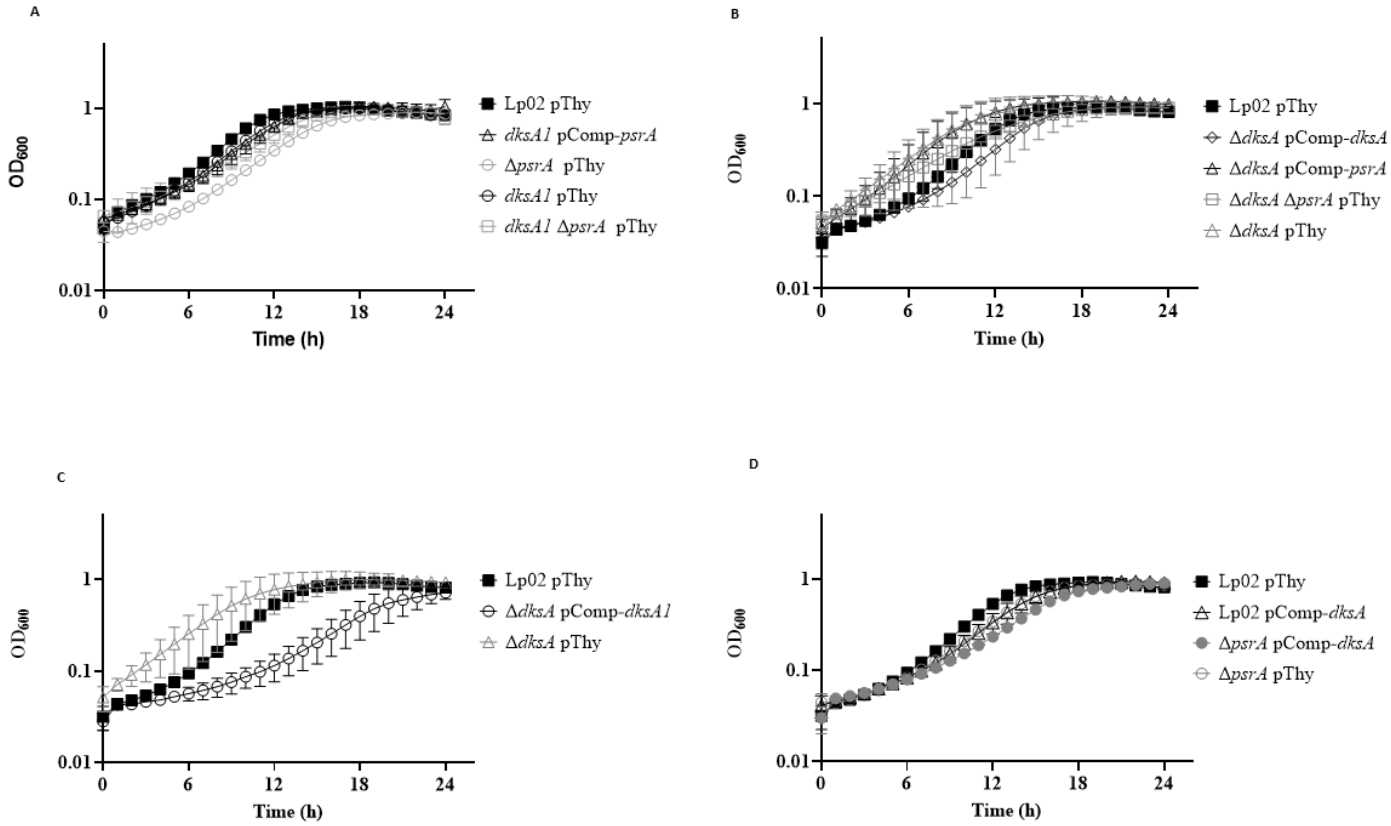

Figure 4: *L. pneumophila in vitro* growth at 37°C is impacted by DksA, PsrA and DksA1. *In vitro* growth kinetics of *L. pneumophila* strains: parental Lp02 and isogenic strains featuring single or combinatorial genetic mutations (Δ*psrA*, Δ*dksA*, *dksA1*) and/or *in-trans* complementation or overexpression of *psrA*, *dksA*, or *dksA1* genes. Plate-grown bacteria were suspended in BYE broth and normalized to initial OD_{600} = 0.15, and growth at 37°C was monitored for OD_{600} hourly for 24 h. Complementation/overexpression was via *in trans* plasmid expression with gene and endogenous promoter cloned into pJB908, pThy is empty control vector pBH6119. Graphs in panels A-D were experiments conducted concurrently, but presented separately for clarity. Error bars are SD across mean of three independent biological replicates with three technical replicates each.

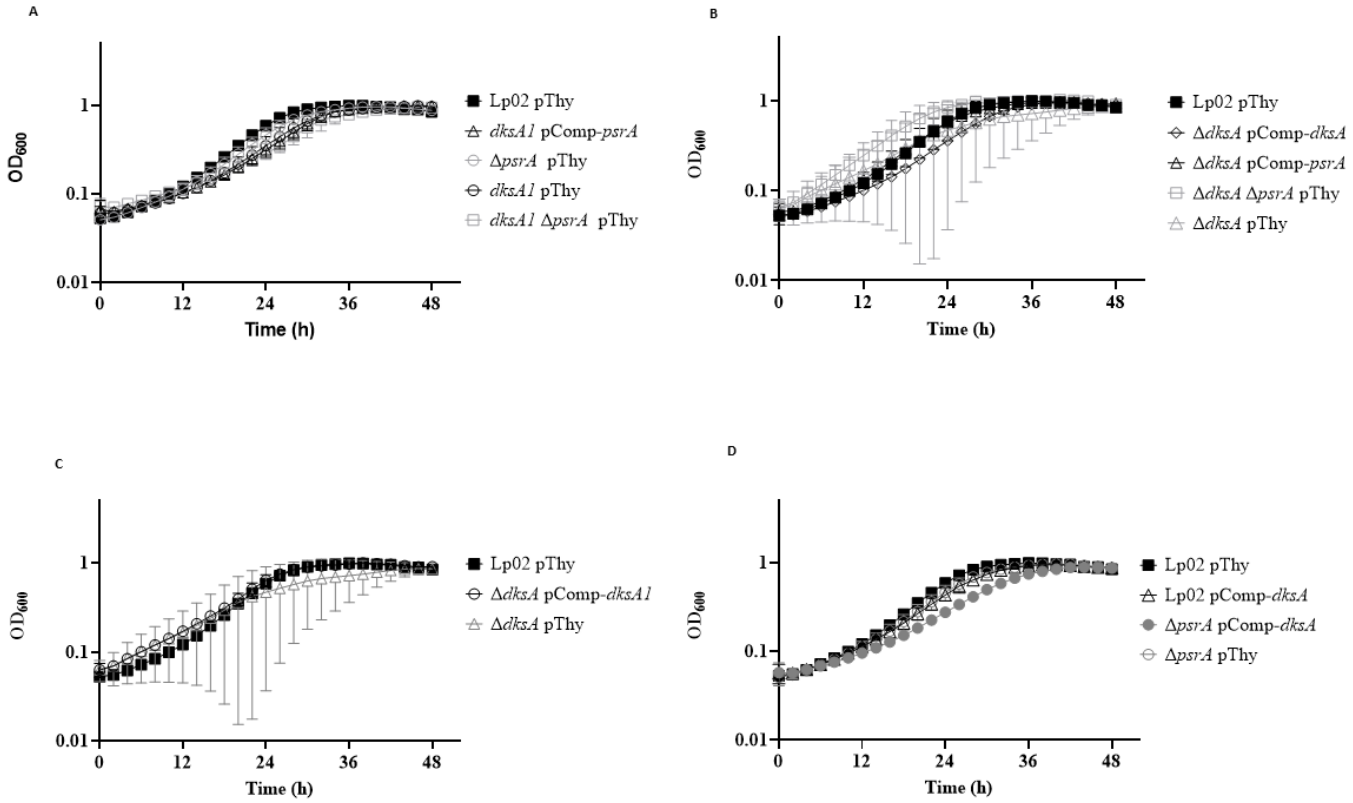

Figure 5: *L. pneumophila in vitro* growth at 25°C is impacted by DksA, PsrA and DksA1. *In vitro* growth kinetics of *L. pneumophila* strains: Parental Lp02 and isogenic strains featuring single or combinatorial genetic mutations (Δ*psrA*, Δ*dksA*, *dksA1*), *in-trans* complementation or overexpression of *psrA*, *dksA* or *dksA1* genes. Lp02 is the parental strain. Complementation/overexpression was via *in trans* plasmid expression with gene and endogenous promoter cloned into pJB908. pThy is empty control vector pBH6119. Plate-grown bacteria were re-suspended in BYE broth and normalized to initial OD_{600} = 0.15, and growth at 25°C was monitored for OD_{600} every 2 h for 48 h. Graphs in panels A-D were experiments conducted concurrently, but presented separately for clarity. Error bars are SD across mean of three independent biological replicates with three technical replicates each.

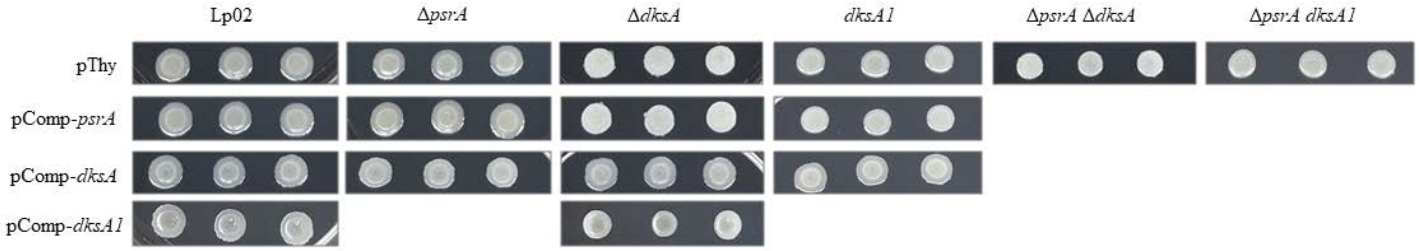

Figure 6: *L. pneumophila* DksA and DksA1, but not PsrA affects colony morphology. Parental Lp02 and isogenic strains featuring single or combinatorial genetic mutations (Δ*psrA*, Δ*dksA*, *dksA1*), and/or *in-trans* complementation or overexpression of *psrA* or *dksA* genes with gene and endogenous promoter cloned into pJB908. pThy is empty control vector pBH6119. Strains were grown on BCYE plates for 3 days and used to generate a bacterial suspension in BYE at OD_{600} = 0.15. 10 µL of the suspension was spotted onto BCYE plates in triplicate then the plates were incubated at 37°C at 5% CO_2 for 4 days prior to being photographed. Images are representative of one of three biological replicates.

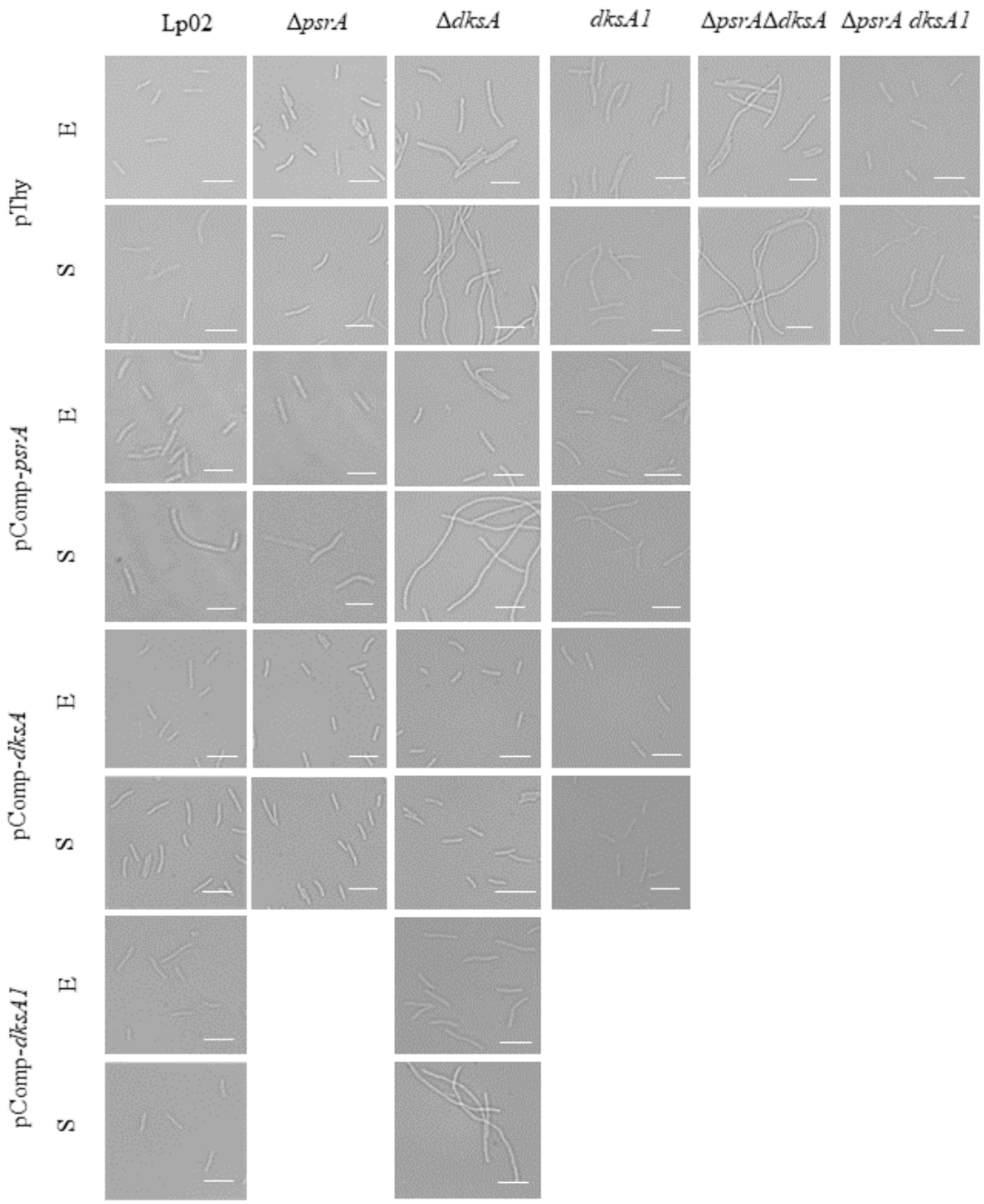

Figure 7*: L. pneumophila* Δ*dksA*, but not *dksA1* or *psrA* cause filamentation. Parental Lp02 and isogenic strains featuring single or combinatorial genetic mutations (Δ*psrA*, Δ*dksA*, *dksA1*), *in-trans* complementation or overexpression of pComp-*psrA*, pComp-*dksA* or pComp-*dksA1* genes were grown on BCYE plates and used to inoculate a dilute suspension of OD_{600} = 0.02 in BYE broth then incubated overnight at 37°C with aeration, to exponential (E) (~18h , OD_{600} = ~0.5) or stationary (S; 24 h after EP) growth phases, then live-mounted on a 2% agarose pad prepared in ddH_2O and imaged on an Axio Observer Z1 inverted microscope (Zeiss) equipped with a glycerol-immersion 150X objective. Representative microscopic images of bacteria from one of three biological replicates. Scale bar is 5 µm.

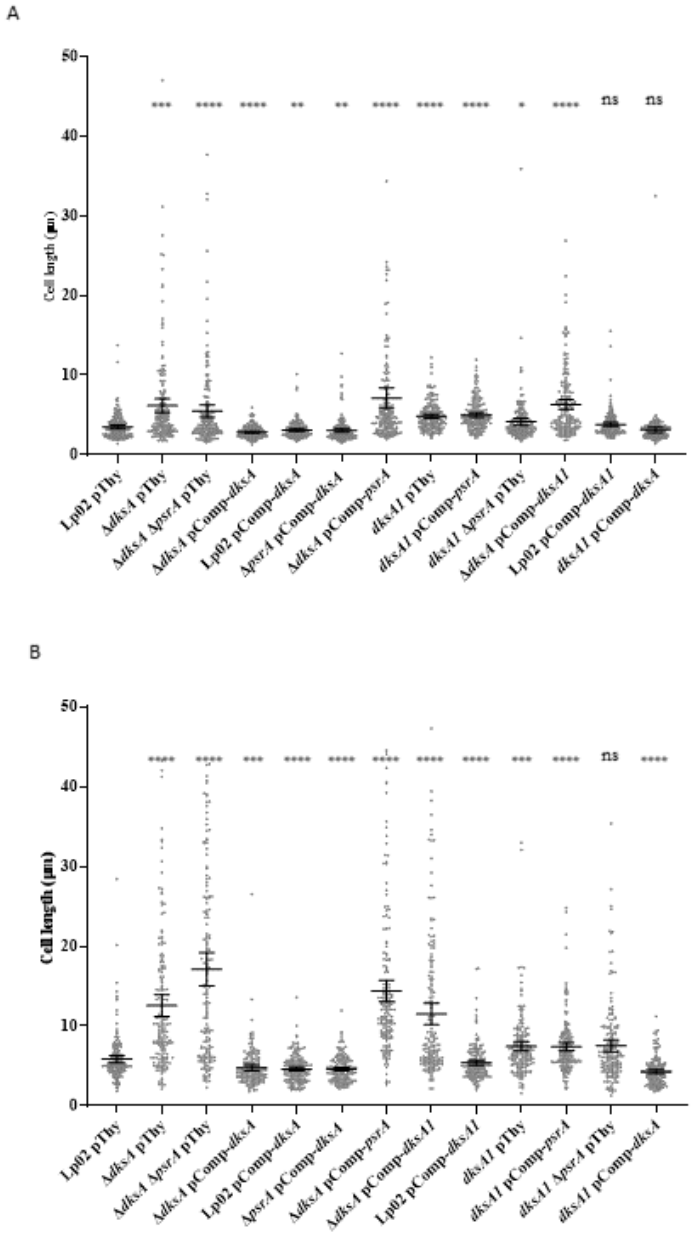

Figure 8*: L. pneumophila* Δ*dksA*, *dksA1*, and *psrA* contribute to cell length regulation. Parental Lp02 and isogenic strains featuring single or combinatorial genetic mutations (Δ*psrA*, Δ*dksA*, *dksA1*), *in-trans* complementation or overexpression of *psrA*, *dksA* or *dksA1* genes were grown from 3-day old plates subcultured to BYE broth at OD_{600} = 0.02 then incubated at 37°C with aeration to (A) exponential (overnight, OD_{600} ~ 0.5) or (B) stationary phases (24 h after exponential phase) then imaged with an Axio Observer Z1 inverted microscope (Zeiss) equipped with a glycerol-immersion 150X objective and individual bacterial cell lengths quantified using the length tool in ImageJ. Where filamentation was evident, only individual cells for which the full length was visible were measured. Data represents >150 individual readings spread equally across three biological replicates. Bar on graph and error bars represents mean and 95% confidence interval, respectively. Statistical significance determined by Student's T-test (*, $p < 0.05$; ** $p < 0.01$; *** $p < 0.001$; **** $p <$ 0,0001; ns, not significant, $p > 0.05$).

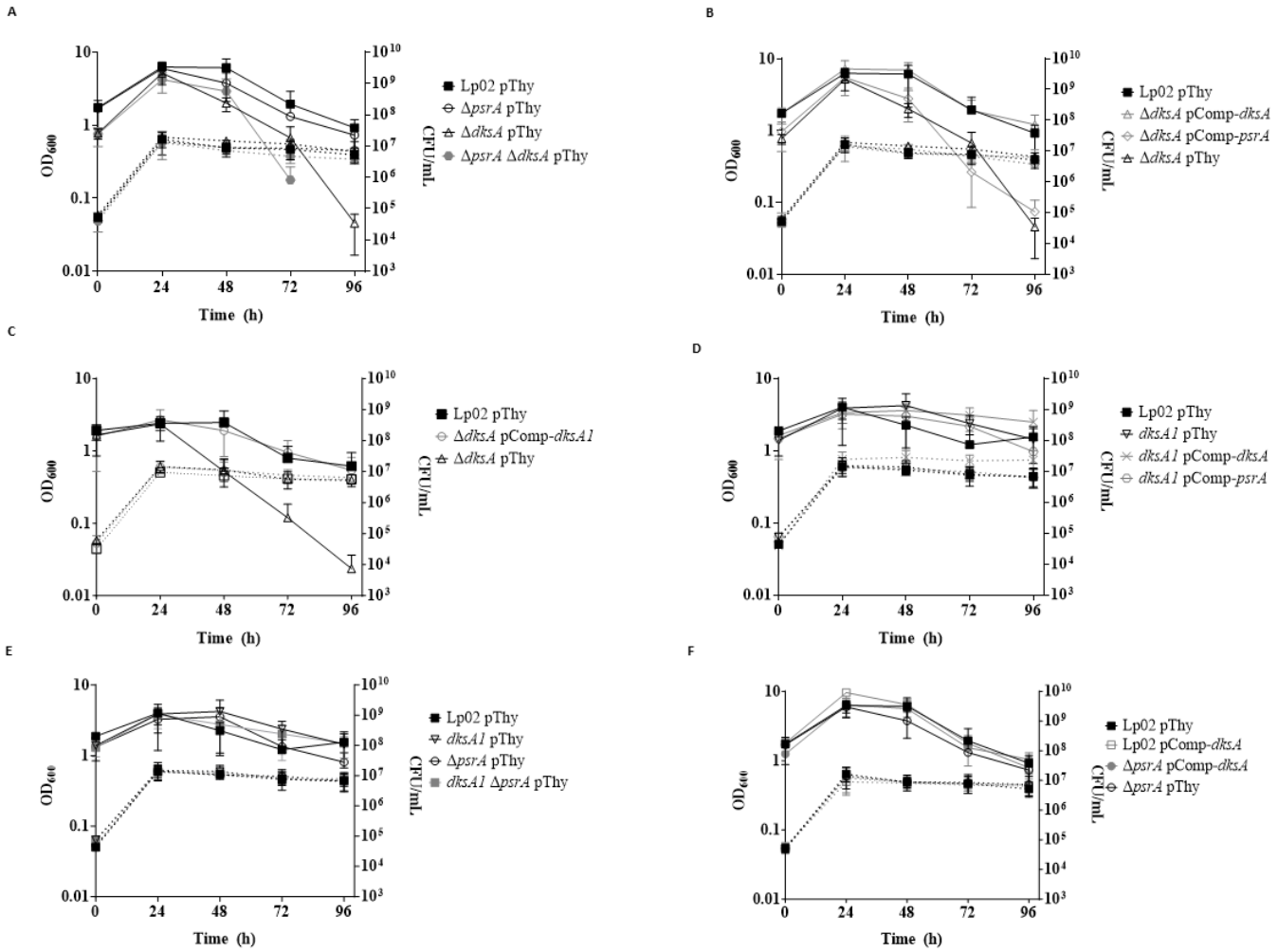

Figure 9: Bacterial culturability in depleted nutrient media is dependent on DksA or DksA1, but not PsrA. Panels (A-F) show *in vitro* growth kinetics of Lp02 and isogenic strains featuring single or combinatorial genetic mutations (Δ*psrA*, Δ*dksA*, *dksA1*), *in-trans* complementation or overexpression of *psrA*, *dksA* or *dksA1* genes, in BYE broth at 37°C for 96 hours with OD_{600} values (dotted lines; left Y axis) and titre enumerated by serial dilution and incubation on BCYE plates (solid lines; right Y axis) at 24 h intervals. Data are presented as mean and SD of three biological replicates. Points were omitted if results could not be calculated (no colonies recovered, below detection limit of ~100 CFU/mL). For ease of comparison, data obtained for select strains (Lp02 pThy, Δ*psrA* pThy, Δ*dksA* pThy, *dksA1* pThy) are shown in more than one panel where panels represent data acquired concurrently.

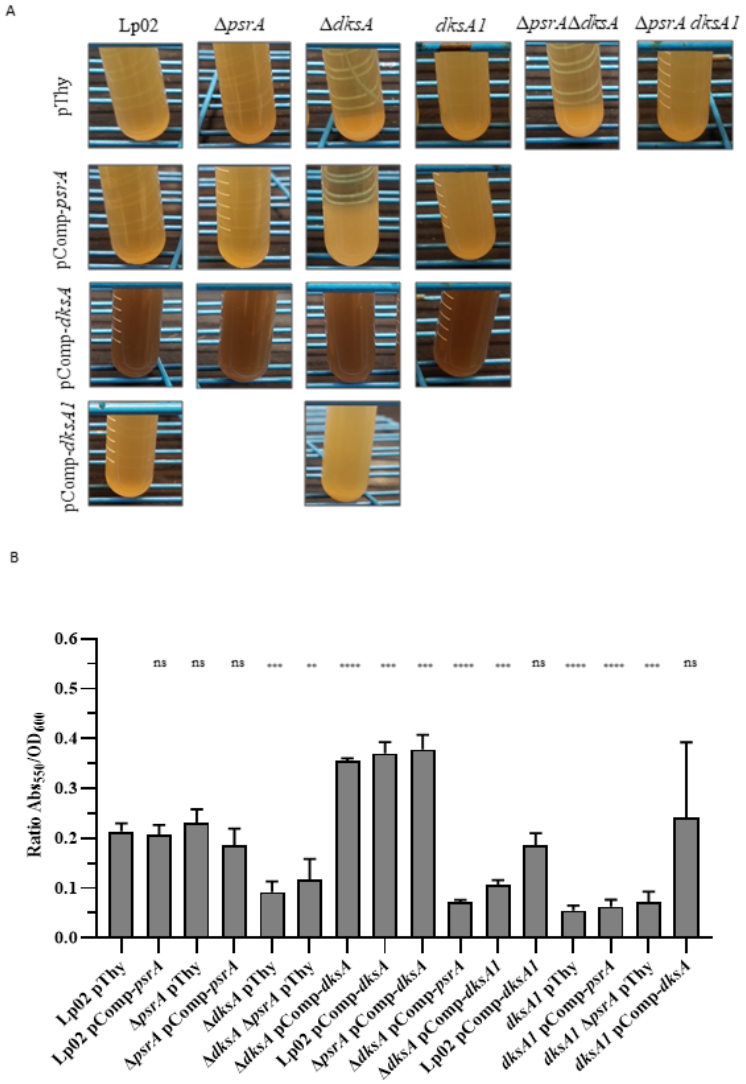

Figure 10: Pigmentation is regulated by DksA, but not PsrA. Parental Lp02 and isogenic strains featuring single or combinatorial genetic mutations (Δ*psrA*, Δ*dksA*, *dksA1*) and/or *in-trans* complementation or overexpression of *psrA, dksA* or *dksA1* genes, were grown on BCYE plates for 3 days and used to generate a 5 mL bacterial suspension (BYE at OD_{600} = 0.15) then incubated at 37°C for 30 h (a) Qualitative observation of pigmentation. After 48 h incubation tubes were set aside for 24 h at room temperature to allow cells to sediment out, then photographed. Representative image of three replicates. (b) Quantification of pigment at 30 h. After 30 h of incubation 1 mL of culture was centrifuged at 20,000 x *g*. The supernatant was measured for pigment levels via absorbance at 550 nm, then the pellet was resuspended in same volume of 1X PBS pH 7.0 to measure cell density via OD_{600}. Readings were taken with a plate reader in a 96 well plate relative to appropriate BYE or PBS blanks. Readings reflect Abs_{550} /OD_{600}. Error bars represent SD across three biological replicates. Statistical significance calculated via Student's T-Test and relative to parental Lp02 pThy, indicated above bars (*, $p < 0.05$, ** $p < 0.01$; *** $p < 0.001$; **** $p < 0{,}0001$; ns, not significant, $p > 0.05$).

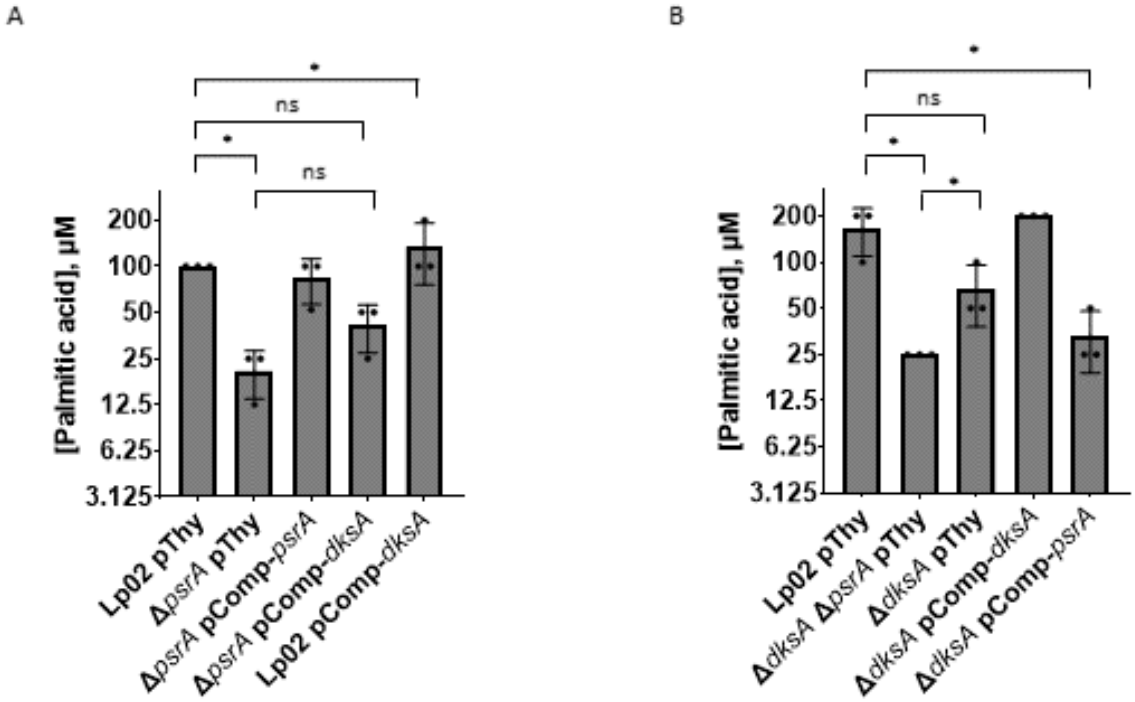

Figure 11: PsrA and DksA influences LCFA-mediated growth inhibition. Parental Lp02 and isogenic strains featuring single or combinatorial genetic mutations (Δ*psrA* and/or Δ*dksA*), and *in-trans* complementation or overexpression of *psrA* or *dksA* genes, grown with and without palmitic acid supplementation (as 40 mM stock dissolved in ethanol) in BYE media normalized to 0.5% ethanol, in a 96-well microplate for 24 h with shaking at 37°C. Inhibition was defined as growth, as assessed by OD_{600} values, of <50% of that of same strain in a BYE + 0.5% ethanol-only control at the end of 24 h. Bars indicate mean of maximum concentration of PA where indicated strain grew >50% of maximum, over three biological replicates with standard deviation indicated. Dots in bars indicate individual replicate values. Panels A and B were conducted separately. Statistical analyses were done using Student's unpaired T test: ns = no significance, * = $p<0.05$.

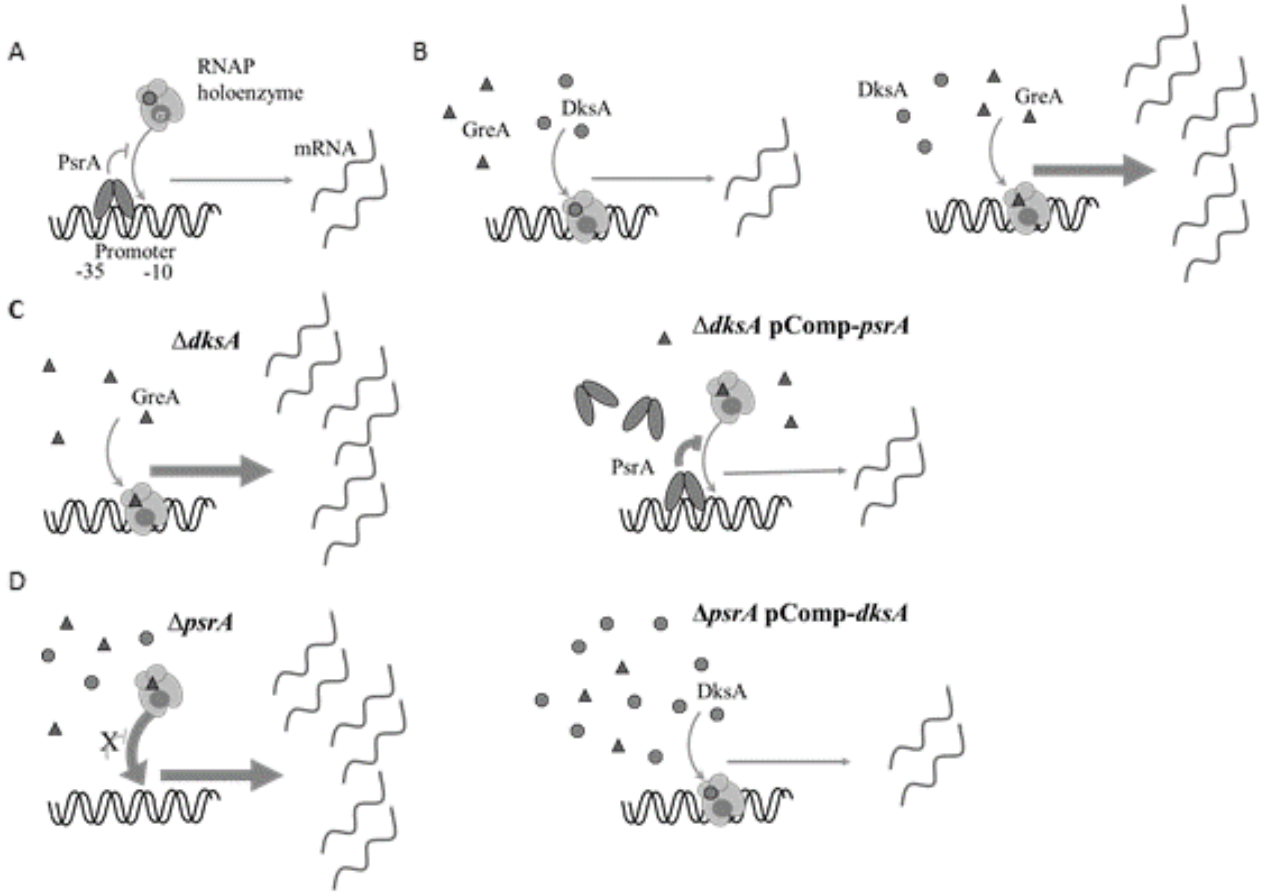

Figure 12: Model of independent mechanisms of DksA and PsrA. A hypothetical promoter is repressed by both PsrA and DksA (A) RNA polymerase (RNAP) holoenzyme is targeted to -10 and -35 boxes by a sigma factor. PsrA (oval dimers) binds a defined site in the promoter and inhibits RNAP recruitment. (B) RNAP binds to GreA (triangles) or DksA (filled octagons) interchangeably, with enhanced transcription initiation rates occurring while bound to GreA versus DksA. (C) In a Δ*dksA* strain, only GreA is available for RNAP thus elevating transcription levels, but *in trans psrA* overexpression generates higher levels of PsrA, strengthening inhibition of RNAP recruitment to compensate. Conversely (D) the Δ*psrA* strain allows uninhibited RNAP-promoter binding, increasing transcription, but this is offset by overexpressing *dksA in trans*, increasing the proportion of RNAP bound to transcription-inhibiting DksA thereby generating the compensatory effect.